Readjustments of a sinuous river during the last 6000 years in northwestern Europe (Cher River, France): From an active meandering river to a stable river course under human forcing

Anaëlle Vayssière, Cyril Castanet, Emmanuèle Gautier, Clément Virmoux, Thomas Depret, Emmanuel Gandouin, Anne-Lise Develle, Fatima Mokadem, Ségolène Saulnier-Copard, Pierre Sabatier, et al.

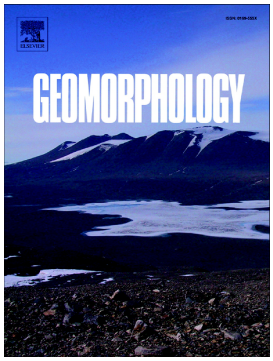

Readjustments of a sinuous river during the last 6000 years in northwestern Europe (Cher River, France): From an active meandering river to a stable river course under human forcing

Anaëlle Vayssiere, Cyril Castanet, Emmanuèle Gautier, Clément Virmoux, Thomas Depret, Emmanuel Gandouin, Anne-Lise Develle, Fatima Mokadem, Ségolène Saulnier-Copard, Pierre Sabatier, Nathalie Carcaud

PII: S0169-555X(20)30368-8

DOI: https://doi.org/10.1016/j.geomorph.2020.107395

Reference: GEOMOR 107395

To appear in: *Geomorphology*

Received date: 27 April 2020

Revised date: 20 August 2020

Accepted date: 20 August 2020

Please cite this article as: A. Vayssiere, C. Castanet, E. Gautier, et al., Readjustments of a sinuous river during the last 6000 years in northwestern Europe (Cher River, France): From an active meandering river to a stable river course under human forcing, *Geomorphology* (2020), https://doi.org/10.1016/j.geomorph.2020.107395

Readjustments of a sinuous river during the last 6000 years in northwestern Europe (Cher River, France): from an active meandering river to a stable river course under human forcing

Anaëlle VAYSSIERE (1), Cyril CASTANET(2), Emmanuèle GAUTIER(3), Clément VIRMOUX (4), Thomas DEPRET(4), Emmanuel GANDOUIN (5), Anne-Lise DEVELLE (6), Fatima MOKADEM(4), Ségolène SAULNIER-COPARD(4), Pierre SABATIER(6), Nathalie CARCAUD(7)

(1)Université Paris 1 Panthéon-Sorbonne, Laboratoire de Géographie Physique, LGP CNRS-UMR 8591, Paris, France. Now at La Rochelle Université, Littoral, Environnement et Sociétés, LIENSS CNRS UMR7266, La Rochelle, France

(2)Université Paris 8 Vincennes-Saint-Denis, Laboratoire de Géographie Physique, LGP CNRS-UMR 8591, Paris, France

(3) Université Paris 1 Panthéon-Sorbonne, Laboratoire de Géographie Physique, LGP CNRS-UMR 8591, Paris, France

(4)Laboratoire de Géographie Physique, LGP CNRS-UMR 8591, Paris, France

(5)Aix- Marseille Univ, Avignon Université, CNRS, IRD, IMBE, Aix-en-Provence, France

(6) Université Savoie Mont Blanc, Environnements, Dynamique et Territoires de Montagne (EDYTEM), CNRS, 73373 Le Bourget du Lac, France

(7)Agrocampus-Ouest, Laboratoire Espace et Sociétés, ESO CNRS-UMR 6590, Angers, France

Abstract:

Palaeomeanders are characteristic features of meandering river floodplains. Some were abandoned several millennia ago and can be used as evidence for past fluvial patterns. Despite many observations of changes undergone by meandering rivers, little is known about long-term morphological adjustment of meanders. This paper reports on investigations conducted in two reaches located in the middle valley of the Cher River (northwestern Europe, France) to examine the readjustments of lowland meanders during the second half of the Holocene. The aim of our study was to provide new insights into the complex dynamics that control low-energy meandering rivers. LiDAR DEM spatial analyses coupled with geophysical surveys and observations of sediments enabled the identification and dating of thirteen palaeomeanders embedded in coarse sediments (sand and gravel) while the whole floodplain is covered by silty overbank deposits. Sedimentological, geochemical and pollen analyses combined with radiocarbon and OSL dating allowed us to reconstruct the chronology of the cutoff and the filling of palaeochannels. No palaeochannels older than *ca* 6000 yr cal. BP, and no palaeochannels younger than the eleventh–thirteenth centuries cal. AD were identified. This allowed us to distinguish

two periods of meandering processes. (1) Our observations demonstrate the multi-millennia persistence of an active meandering pattern in a context of land use changes (*ca* 6000 yr cal. BP-eleventh–thirteenth centuries cal. AD). The preserved mobility of the river can be mainly interpreted as the result of the low cohesiveness of the bank material. Too few fine sediments were delivered during the proto-historical and historical periods to help stabilize the river course. (2) Following the eleventh–thirteenth centuries cal. AD, the fluvial system underwent a laterally stable phase. The many medieval and modern hydraulic engineering works reduced the specific stream power and prevented lateral erosion. The drastic decrease in the river's capacity to generate new meanders resulted in the disappearance of floodplain lakes and loss of habitat diversity.

Keywords: Palaeochannel, meanders, floodplain, channel mobility, Holocene, Cher River

1. Introduction

Palaeomeanders abandoned several millennia ago are considered as evidence for past fluvial patterns (e.g., Kozarski and Rotnicki, 1977; Salvador and Berger, 2014; Toonen et al., 2012). The coexistence of meanders and palaeomeanders in floodplains is closely related to lateral dynamics such as lateral accretion through bar formation, concave bank erosion, neck or chute cutoff of meander bends (Allen, 1965; Fisk, 1947; Petts and Amoros, 1996) and, to a lesser extent, vertical dynamics such as entrenchment of the riverbed.

An abundant literature is devoted to the study of river metamorphosis as a consequence of the strong climatic forcing in the Quaternary period (e.g., Houben, 2003; Mol et al., 2000; Vandenberghe, 2008, 2003, 1993; Vandenberghe et al., 1994), whereas little is known about the functioning of meanders as a perennial fluvial pattern during interglacial conditions like in the Holocene (e.g., Brooks, 2003; Candel et al., 2018; Lewin and Macklin, 2010). However, meanders and associated palaeomeanders are widespread features of existing rivers of northwestern Europe. Long-term studies of meanders will improve our understanding of these contemporary rivers and be useful for future ecosystem management (Brown et al., 2018; Lespez et al., 2015).

Palaeomeanders are difficult to interpret as palaeohydrological fluvial dynamics for three main reasons:

(1) During the Holocene, and mainly since the second half of the Holocene in western Europe, fluvial geomorphology was affected by anthropogenic forcing that implies a significant

change in the external controls on river catchments (Brown et al., 2018; Carcaud, 2004; Erkens et al., 2009; Hoffmann et al., 2009; Notebaert and Verstraeten, 2010; Pastre et al., 2002). The complexity is reinforced because human pressure on fluvial landforms and the environment is a nonlinear process punctuated by tipping points (Brown et al., 2013; Lespez et al., 2015; Notebaert et al., 2018)

(2) Once they are abandoned, palaeomeanders are subject to different hydrological processes that alter their original shape to varying degrees (Toonen et al., 2012). A cutoff is followed by the formation of an alluvial plug at the upstream inlet of the abandoned channel, resulting in the formation of an oxbow lake (Allen, 1965; Constantine et al., 2010; Dieras, 2013; Dieras et al., 2013; Gautier et al., 2010, 2007). Depending on their geometry and hydrological connection with the main river, abandoned channels may function as lotic lakes (connected by an upstream inlet), backwater lakes (connected to the active channel by a downstream outlet), or lentic passive lakes (mainly connected to underground water and disconnected from the main river) (Citterio and Piégay, 2000, 2009; Gautier et al., 2010, 2007; Hohensinner et al., 2004). Next, the palaeochannel changes from an aquatic to a terrestrial environment. The pace and nature of the filling of palaeomeanders depend on the flood regime (sediment supply) as well as on local controls such as distance from the main channel, vegetation, diversion angle and water table level (Citterio and Piégay, 2009, 2000; Constantine et al., 2010; Dépret et al., 2017a; Gautier et al., 2010, 2007; Hooke, 1995; Toonen et al., 2012). The difference in the ways palaeochannels change (energy of the flow, sedimentation rate, persistence of an aquatic environment) over time is caused by the diversity of sediment sources and hydrological connectivity with the main channel (Toonen et al., 2012).

(3) Meander cutoff as a result of channel migration is an inherent process of meandering rivers that do not need to be exogenously triggered because sinuous rivers tend to cut themselves off (Hooke, 1987; Stølum, 1996). As a consequence, the external controlling factors on fluvial landforms are not easy to distinguish from self-adjustment.

The middle Cher valley is a lowland area with gentle slopes and a wide floodplain that enables the preservation of numerous silted-up palaeomeanders that were identified through topographic analyses

of the floodplain. Thirteen cutoffs were dated from the Middle Holocene until the historic period, suggesting active meandering processes (Vayssière, 2018; Vayssière et al., 2019, 2016). Consistent information on cutoff chronology coupled with changes in oxbow lakes can be obtained by studying former meanders (location, age and filling). This case study offered a favorable context for a multi-disciplinary analysis (mainly based on geomorphology but also on geochemistry, sedimentology and pollen analyses) of appropriate fluvial archives to understand the long-term adjustments of floodplains in a context of land-use changes.

The study of the Cher River valley provided a relevant example of a sinuous river associated with a very large number of palaeomeanders denoting the shifting of the watercourse and which, paradoxically, has displayed very low mobility for the last 200 yr (Dépret et al., 2017b). The causes of this recent stability of the Cher River meanders were investigated (Dépret, 2013, 2014; Dépret et al., 2015, 2017b) and these studies are extremely useful as they are analogous and provide a lot of information about recent hydrological controls on the morphogenesis of the Cher River. These investigations conducted in the Cher River valley improve our understanding of the complex dynamics that control meandering rivers during the second half of the Holocene by assessing the morphodynamic changes of a lowland sinuous river and to understand the extent to which the changes are linked to the climatic and anthropogenic context or should rather be considered as self-adjustment.

The main objectives of the study were to (1) identify and map palaeomeanders in two reaches of the middle Cher River valley and to propose a cutoff chronology, (2) analyze in detail the sedimentary fill of the palaeochannels, (3) reconstruct the palaeogeography of the channel pattern and mobility and (4) propose driving factors based on the information provided by all the previous objectives but also based on our knowledge of human practices and climate oscillations during the Holocene and on current hydrological controls on morphogenesis of the Cher River. Studying two different reaches also helped distinguish local and basin-scale factors.

2. Regional setting

The Cher River is one of the main tributaries of the Loire River, which is the longest watercourse in

France (Fig. 1). The Cher River is 368 km long with a catchment area of 14,000 km². The highest point along its course is 710 m a.s.l. and the lowest is 38 m a.s.l. at the junction with the Loire River. The upper basin is located in the Massif Central, which is mainly composed of crystalline rocks (Fig. 2). The middle and the lower valleys correspond to the Triassic, Jurassic and Cretaceous limestones south of the sedimentary basin of Paris (Fig. 2).

Recent investigations we conducted in the Cher River valley based on floodplain archives allowed us to reconstruct the Lateglacial geomorphological trajectory (Vayssière et al., 2019). Climatic oscillations during the Pleniglacial and Lateglacial periods are generally associated with changes in fluvial morphology and processes. During the early Lateglacial, fluvial morphology corresponded to a transitional pattern composed of at least two straight channels including one main branch and lateral channel(s). During the Bölling and Allerød interstadials, secondary channels were abandoned and filled with organic silt and peaty deposits (Vayssière et al., 2019). The Holocene is characterized by a more temperate climate than in the Lateglacial period. Nevertheless, the past ten millennia were punctuated by climate fluctuations that likely affected fluvial systems. During the second half of the Holocene fluvial dynamics became more complex because of human forcing.

Extensive archaeological surveys of the rural habitat during the Iron Age and the Gallo-Roman era (Gandini, 2006) and the river management during the medieval and modern periods (Serna, 2013) suggest that the Cher River valley has been settled for a long time. This hypothesis is supported by the results of palaeoecological studies conducted in the floodplain and adjacent small catchments. These investigations revealed that the first anthropogenic fires occurred during the transition from the Middle to the Late Neolithic from 5150–5050 cal. BP (Vannière and Laggoun-Defarge, 2002; Vannière and Martineau, 2005). Currently, the Cher River has numerous hydraulic engineering works (Serna, 2013). The riverbed and the floodplain are also disturbed as the result of several gravel extractions (Cossalter, 2011; Dépret, 2014; Serna, 2013).

The present study focused on two reaches: Bigny and Thénioux (Fig.1). The choice of the two sites was based on the identification of many Holocene palaeomeanders. Furthermore, they are located very

close to sites whose history is abundantly documented (mentioned as "reach 2" and "reach 3" in Dépret et al., 2017b; 2015). These two reaches show a concentration of hydraulic engineering works, human settlements and activities that have affected both the riverbed and the floodplain. The engineering structures (mills, fluvial ports, dams, canals, bridges, proto-industrial sites and gravel extractions) have been present since the central Middle Ages (Cossalter, 2011; Dépret, 2014; Serna, 2013).

The Bigny area is located eight kilometers downstream of the 'reach 2' described in Dépret et al. (2017b; 2015). The drainage area at this site is 4100 km² with a valley slope of 0.00083 $m.m^{-1}$ (Table 1). The geology in the area consists of Middle Jurassic and upper Eocene and Oligocene clays and limestone (Lablanche et al., 1994; Lablanche and Desprez, 1984). A characteristic feature of this reach is the large number of sinuous palaeochannels (Vayssière, 2018; Vayssière et al., 2016).

The Thénioux area is located about 70 km downstream of Bigny and is adjacent to the 'reach 3' described in Dépret et al. (2017b; 2015). The river drains an area of 9070 km². The valley slope is slightly less steep than the upstream study area (0.000695 $m.m^{-1}$) (Table 1). The bedrock consists of Upper Cretaceous formations (Manivit et al., 1994). The Thénioux site is located immediately downstream of the confluence with the Yèvre and Arnon rivers, two of the main tributaries of the Cher River. A characteristic feature of this reach is the diversity of inherited fluvial landforms. Indeed, the floodplain is occupied by wide straight palaeochannels inherited from the Lateglacial period mentioned above (Vayssière et al., 2019) and by the Holocene meander belt.

3. Materials and methods

3.1. Reconstruction of the floodplain sedimentary architecture and palaeohydrographic mapping

The approach we used in the Cher floodplain consisted of spatial analysis using a LiDAR (Light Detection And Ranging) DEM (Digital Elevation Model) coupled with geophysical surveys and sedimentary observations.

The LiDAR DEM provides an accurate topographic dataset suitable for identifying former fluvial landforms such as abandoned channels and bars (e.g., Notebaert et al., 2009). The 1 m² pixel LiDAR DEM data were acquired in the Cher River valley between 2009 and 2011 and has a mean vertical accuracy of +/- 0.089 m (minimum: +/- 0.15 m). The whole surface of the floodplain is covered by 1 km × 1 km geo-referenced tiles. The tiles corresponding to our study areas were merged using GIS software (ArcGIS 10.4). Inherited landforms were digitized and mapped by correcting the longitudinal inclination of the valley floor. The method consists of subtracting a DEM whose slope corresponds to the slope of the valley from the original DEM. The methods are detailed in Vayssière et al. (2019) and adapted from the method developed for the Burgundy Loire valley (Steinmann, 2015; Steinmann et al., 2017). By displaying their relative elevation, inherited landforms were easily identified, digitized and mapped.

To account for the lateral variability of alluvial fill, extended cross-sections of the valley bottom were examined including boreholes, outcrops, and the results of geophysical surveys (Fig. 3). A total of 102 mechanical and manual boreholes were drilled, of which 35 in the Bigny area and 67 in the Thénioux area. Two outcrops were investigated in the Thénioux reach. Lithofacies were logged using Miall terminology (Miall, 1996). Nineteen additional stratigraphic logs from BSS-BRGM (*Bureau des Recherches Géologiques et Minières*, Mining and Geological Research Institute) database and 35 logs from CEREMA (*Centre d'études et d'expertise sur les risques, l'environnement, la mobilité et l'aménagement*, Centre for Studies and Expertise on Risks, Environment, Mobility and Development) were studied.

Geophysical surveys using electrical resistivity tomography (ERT) were conducted to identify palaeochannels and former secondary channels. ERT depicts the distribution of the subsoil electrical resistivity values (expressed in ohm.m) (Loke, 2000; Marescot, 2006). Resistivity varies with the porosity, degree of water saturation, dissolved salt content and to a lesser extent, temperature (Loke, 2000). It is a suitable tool to assess the geometry of palaeochannels we have cored because their fill generally consists in low-resistivity sediment (silt and clay). ERT was carried out using an ABEM Terrameter LS sensor with 64 electrodes spaced 2 m apart. Three two-dimensional 766 m, 223 m and

76 m long cross sections were surveyed at Thénioux and one 1040 m long cross section was surveyed at Bigny.

3.2. Palaeochannel infill analysis

Channel cutoffs have created fluvio-lacustrine environments in the floodplain. Seven cores were collected using a Cobra TT and a SEDIDRILL mechanical auger in pools of former channels that are favorable environments for high-resolution sedimentary records and organic preservation (Ejarque et al., 2014; Erskine et al., 1992; Salvador, 2005; Salvador et al., 2004; Salvador and Berger, 2014; Toonen et al., 2012). The deposits were studied in order to reconstruct the environmental conditions that prevailed following the cutoff. Cores collected from palaeochannels are suitable for use with a multi-parameter approach helping to estimate the energy of the flow, the sediment rate, the source and the transport processes of the sediment and the vegetation history.

3.2.1. Grain size analyses

Grain size analysis was carried out on samples taken at 5- or 10-cm intervals depending on the vertical variability of sedimentary facies. Organic matter was removed from the samples using hydrogen peroxide (35%). Sediment samples were dispersed with hexametaphosphate sodium (5‰). The grain size distribution (ranging from 0.04 µm to 2000 µm) was measured by laser diffraction with a Beckman-Coulter LS230. Grain size of coarse material (>2 mm) was determined using sieves ranging from 2 mm to 12 mm. Grain size indices were calculated using the GRADISTAT 8.0 program (Blott and Pye, 2001). The grain size scale adopted in this study followed that of Konert and Vandenberghe (1997), Udden (1914) and Wentworth (1922). The transport and sedimentation of fluvial deposits were interpreted using the Passega CM diagram including the D_{50} and D_{99} diameter of the grain-size distribution of each sample (Passega, 1957). These indices were calculated using the Bunte and Abt (2001) equation:

$$D_x = 10^{[(\log(x2)-\log(x1))\left(\frac{x-y1}{y2-y1}\right)+x1]} \quad (1)$$

where *x* is the percentile value, *y1* and *y2* are frequency values framing *x*, and *x1* and *x2* are grain diameters associated with *y1* and *y2*.

3.2.2. Geochemistry and core scanning

Additional geochemical analyses were conducted on core BRD12 (Figs. 4 and 5). Geochemical signals provide information on the origin of the deposit. Total carbon (TC), total organic carbon (TOC) and total nitrogen (TN) were analyzed with a Thermo Scientific Flash 2000 CHNS analyzer. The relative contents of major elements were analyzed using x-ray fluorescence (XRF) at high resolution (1 cm sampling step) on the surface of the sediment core with an Avaatech Core Scanner (EDYTEM Laboratory, CNRS-University Savoie Mont Blanc). The x-ray beam was generated with a rhodium anode and a 125 µm beryllium window. The split core surface was first covered with 4 µm-thick Ultralene plastic film. Element intensities are expressed in counts per second (cps). Settings were adjusted to 10 kV and 1 mA for 20 s to detect Si, Ca, Al, Fe, Ti, K, Mn, and S. For heavier elements (i.e., Sr, Rb, Zr, Br, and Pb), measurements were taken at 30 kV and 0.75 mA for 30 s. This provides the relative abundance of each element. The present study used K as the detrital signal, mainly present in clay minerals, Ca as detrital carbonated deposition and/or carbonate precipitation signal, and Mn as precipitation of manganese oxide signal related to oxygenation processes (Sabatier et al., 2017). If we assume that the K content is related to fine terrigenous inputs (Sabatier et al., 2017), the Si/K and Ca/K ratios could be interpreted as biogenic silica (Brisset et al., 2012) and palustrine carbonate precipitation (Bajard et al., 2016), respectively.

3.2.3. Palynology

Pollen analyses were also carried out on the core BRD12, which corresponds to the longest deposition period and therefore was determined to be the most appropriate for a diachronic study. Pollen was extracted using a standard protocol (Faegri et al., 2000). A minimum of 300 pollen grains per sample were identified under a transmission light microscope at ×500 magnification and the results are expressed as percentages of total terrestrial vascular pollen. In this study, pollen types were identified according to Moore (1991) and Reille, (1999). Riparian forest taxa including *Alnus*, *Fraxinus* and *Salix* pollen were excluded from the main pollen sum as they are usually over-represented in sediments from alluvial plains. Pollen assemblage zones (RD12-paz) were designed with the Rioja package (Juggins, 2017) using a depth-constrained cluster analysis (CONISS algorithm) in R software

(R Core Team, 2018 https://www.R-project.org). Taxa were then grouped in eight ecological categories: Upland trees and shrubs, Riparian forest, Crops (cultivated plants), Apophytes (any taxa growing on disturbed land), other apothytes (plant families with many probable apophytes), Herbs, Aquatic (Hydrophylous and Hygrophylous plants) and Ferns.

3.3. Chronology of fluvial deposits and cutoffs

The chronology of fluvial deposits was also based on 36 radiocarbon ages of organic material sampled as much as possible within the downstream pool of the palaeochannel (Table 2). Basal parts of the fine and organic fill deposited within the palaeomeanders overlaying the sandy and/or gravelly layer were dated in order to provide the age of transition to a lentic environment. This age is considered as a limit before which the cutoff occurred. Radiocarbon ages were calibrated using the OxCal v4.3.2 (Bronk Ramsey, 2009) according to the IntCal13 atmospheric curve (Reimer et al., 2013). When pollen data are compared with the regional vegetation history, they can provide valuable bio-chronostratigraphic evidence (Cyprien et al., 2004; Visset et al., 2008), which increases the reliability of the radiocarbon chronology.

For optically stimulated luminescence (OSL) measurements, seven samples were collected during outcrop surveys in a concave eroding bank in Thénioux (Table 3). The samples for luminescence measurements were collected by inserting sampling tubes into the bank. To enable dose rate characterization, sediments were also collected within a 30 cm radius of each sample. A portion of each sample was kept for grain size analyses. Pure quartz was extracted from each sample for De (Equivalent dose) measurements. In the laboratory darkroom, the sample was first treated with 10% HCl and 30% H_2O_2 to remove organic materials and carbonates, respectively. After grain size separation, the 90-150 µm fraction was relatively abundant. As a result, this fraction was chosen for De determination. Heavy metals were removed by flotation in sodium polytungstate. The grains were treated with HF acid (40%) for 45-90 min, then with 10% HCl acid to remove fluoride precipitates. The purity of the quartz was checked with IR stimulation with negligible IRSL. Quartz OSL was measured using an automated Risø TL/OSL-20 reader. A blue LED (λ=470±20 nm) stimulation source was used for 40 s at 130°C. Irradiation was carried out using a 90Sr/90Y beta source built into the

reader. The OSL signal was detected via a 9235QA photomultiplier tube through a U-340 filter. OSL signals from the first 0.64 s stimulation were used to build the growth curve after background subtraction. The single aliquot regenerative dose (SAR) protocol was used to measure De (Murray and Olley, 2002; Murray and Wintle, 2000). Preheat temperatures of 240°C for 10 s and 160°C were chosen as cut heat temperatures. The final De is the average De of all the aliquots, and the error of the final De is the standard error of the De distribution.

The quartz OSL was dominated by fast components. Recycling ratios were between 0.90 and 1.1. Recuperation was negligible. The beta and gamma contributions to the dose rate were calculated from concentrations of U, Th, and K measured by the ICP-MS and ICP-AES after hydrofluoric-nitric-perchloric acid digestion (10% error assumed). The cosmic ray dose rate for each sample was estimated as a function of depth, altitude and geomagnetic latitude (Prescott and Hutton, 1994). The final OSL age (in ka, 1000 yr) is then: De/Dose-rate.

3.4. Assessment of sedimentation rates

Sedimentation rates (in $cm.yr^{-1}$) were defined with radiocarbon ages by using the median probability plotted during the calibration (see section 3.3). These chronological markers refer to periods of time that are identified by the thickness of the sediment layer between each. The reliability of the sedimentation rate reconstructions depends on the number of chronological controls and on their distribution along the core.

4. Results

4.1. Spatial distribution of former meanders

Thirteen meanders in Bigny and ten in Thénioux were identified on the basis of LiDAR DEM analyses (Fig. 3). An additional former meander (outcrop1: TRD1-Ch1) and lateral accretion facies (outcrop 2: TRG-LA) were identified at Thénioux at the base of outcrop surveys, (Figs. 3, 4 and 5). Three main types of sedimentary bodies can be distinguished in the representative cross section of both study areas (Fig. 4):

- Coarse sedimentary bodies composed of sand and gravel that appear to comprise most of the floodplain fill. These were interpreted as lateral accretion deposits (LA-Sm, LA-Gcm, LA-Gmm) according to Miall (1996) terminology;
- Fluvio-palustrine deposits recorded in palaeochannels converted into floodplain ponds or lakes (CH-Fsm);
- Overbank silty deposits (FF-Fsm) covering the entire floodplain.

4.1.1. Upstream reach: Bigny

The width of the floodplain at Bigny is 1.22 km. Boreholes L1 and L2 provided precise information about the depth of the bedrock, which varies between 6.2 and 6.9 m (Fig. 4A and B). Several former meanders were identified. All these abandoned channels have evolved towards terrestrial environments, but one corresponded to a pond area (BRD9) still connected with the groundwater. The topography is weakly contrasted except for one distinct level identified on the margins of the floodplain (Fig. 4A and B). Borehole L6 showed that the top of this sedimentary body is composed of carbonated mud with shells overlapping sandy alluvium. This topographic level could correspond to a small terrace, however, no palaeochannel has been clearly identified through the LiDAR DEM analyses, the boreholes or the geophysical survey.

The central part of the floodplain is mostly flat except for slight depressions caused by the presence of former channels. Two distinct sets of resistivity values were identified during the ERT survey. On the one hand, a portion of the floodplain is characterized by high resistivity values (90–490 ohm.m) contrasting with the low resistivity of the bedrock. This part of the valley is mainly composed of sand and gravels deposited because of the successive deposition of point bars (LA-Sm, LA-Gcm, LA-Gmm) identified from 0 m (L1) to 1.2 m (L2, L3, L4 and L5) in depth (Fig. 4A). The upper part of the Holocene fill consists of overbank silt and clay deposits (FF-Fsm) whose thickness is about 1.2 m (L2, L3, L4 and L5). The other portion is characterized by low resistivity values (9–90 ohm.m) because of its finer texture. The lowest values identify the palaeochannel infill (CH). In this way, three main former meanders were identified. The oldest (BRD9) was abandoned at 5272–4867 yr cal. BP. Two younger palaeomeanders (BRD10 and BRD11) were abandoned around 1346–1522 and 1303–1184 yr

cal. BP. Smaller palaeochannels (BRD12; L4 and L5, Fig. 4A) are interpreted as chute channels associated with former meander migrations. BRD12 provided material suitable for radiocarbon dating and showed that the infilling process lasted from 6179–5928 yr cal. BP to 789–683 yr cal. BP. The palaeomeander fill is covered by a silty overbank deposit (CH/FF-Fsm). This aggradation began in the historic period, around 2114-1901 yr cal. BP (Poz-77937) in the palaeochannel BRD9 and before 1864-1639 (Poz-75193) and 1070-938 (DeA- 8890) yr cal. BP in BRD12 and BRD11, respectively.

4.1.2. Downstream reach: Thénioux

The width of the floodplain at Thénioux is about 2.75 km. According to the boreholes, the substratum is at a depth of 6.4 m in the center of the floodplain (L3) and at a depth of 3.5 m at the foot of the northeast slope (Fig. 4C). Part of the valley bottom is occupied by landforms inherited from the Lateglacial Period consisting in elongated slightly elevated areas –which we refer to as "*montilles*"- separated by straight palaeochannels abandoned during Bölling and Allerød interstadials (Vayssière et al., 2019). The other part of the valley bottom is occupied by the Holocene meander belt located at the same topographic level as Pleistocene deposits denoting the lack of conspicuous incision at the transition between the two periods (Fig. 4C). The synthetic cross section includes two outcrop sites. The first site corresponds to a concave area where lateral erosion is clearing out older deposits (outcrop 1). The second site corresponds to a quarry where several outcrops were analyzed (outcrop 2). A coarse sedimentary body composed of sand and gravel interpreted as lateral accretion deposits (LA-Sm, LA-Gcm, LA-Gmm) was observed from a depth of 0.45 (L3) to 0.6 m (L2) (Fig. 4C). One meander cutoff occurring around 3453–3347 yr cal. BP was identified by borehole TRG1. On the right bank, one meandering palaeochannel (TRDCh-1) was identified by examining outcrop 1. Its cutoff occurred around 2860 ± 249 yr cal. BP (OSL ages). It was filled in with a silty-clay accumulation (CH-Fl) and sandy deposition (CH-Sh) during a period of a few centuries (2151 ± 173 yr cal. BP, OSL ages). On the left bank of the river, scroll bars and lateral accretion facies (TRG-LA) were identified by examining outcrop 2 showing several stages in the southwestward migration of a meander between 1702 and 1184 yr cal. BP based on four radiocarbon ages (DeA- 8895; Beta – 440280; Beta – 440281; Beta – 440282) (Table 2). The upper part of the Holocene fill consists of overbank silt and clay

deposits (FF-Fsm) whose thickness varies between 0.5 in the floodplain and 1.5 m in the palaeochannels. This deposition associated with overbank flows may have occurred at the end of the proto-historical period and during historical times. The radiocarbon age of charcoal embedded in these silty deposits showed that the deposition occurred around 925–785 yr cal. BP above the filled paleochannel TRDCh-1.

4.2. Chronology of cutoffs

Seven palaeochannel cutoffs were dated in Bigny and seven in Thénioux by coupling radiocarbon and OSL (Figs. 5 and 6). No sinuous palaeochannel cutoff older than *ca* 6000 yr cal. BP was identified despite observations using boreholes and the outcrop survey. Some palaeomeanders identified through the topographic analyses have not been dated (Fig. 5) because they did not have organic matter suitable for radiocarbon dating.

In the Bigny study area, the oldest dated channel (BRD9) was abandoned 5272–4867 yr cal. BP (Subboreal/beginning of the late Neolithic). Another channel (BRD7) was abandoned around 3569–3410 yr cal. BP (Subatlantic/Bronze Age). The chute channel (BRD12) was completely disconnected around 2774–2721 yr cal. BP (Subatlantic/beginning of the Iron Age). Other dated former channels were abandoned in historical times. Three of them (BRD10, BRD8, BRD11) were cut between 1522 and 1184 yr cal. BP (late antiquity/central Middle Ages). The location of the abandoned channel BRD12 in relation to the more recent palaeomeander BRD10 raises questions about the age of the latter. It seems paradoxical that a younger meander is more distant from the existing channel. It is possible that the palaeomeander BRD10 was older but reoccupied shortly before 1522-1346 cal. BP without reworking the floodplain deposits. Indeed reoccupation of a pre-existing channel segment can occur without implying the development of a new meander (Gottesfeld and Johnson Gottesfeld, 1990).

The youngest dated channel (BRG1) was probably abandoned during the eleventh–thirteenth centuries cal. AD (930–796 yr cal. BP). It can be assumed that BRD8, BRD11, and BRG1 were active simultaneously.

In the Thénioux study area, two cutoffs (TRG5 and TRG3) were identified between *ca* 6000 and 4500

yr cal. BP (Subboreal/Middle and Late Neolithic). Two abandonments were identified (TRG1, TRG4) at the beginning of the Subatlantic period (late Bronze Age), around 3500–3000 yr cal. BP. OSL ages indicating that the palaeomeander TRD-Ch1 was abandoned before 2860 ± 249 yr cal. BP (3109–2611 yr cal. BP). One historical channel was cut around 1543–1409 yr cal. BP (late antiquity/early Middle Ages). The successive deposition of point bars (outcrop 2) were established between 1702 and 1184 yr cal. BP (TRG-LA), associated with several stages of migration of a meander that could be TRG2.

4.3. Main steps of sedimentary filling of the palaeochannels studied

The study of seven cores collected in palaeomeanders in Bigny provided information on the environmental changes that took place after abandonment. These analyses are based on grain size measurements and sedimentation rates derived from radiocarbon ages. Three main stratigraphic units (MSUs) were characterized (Fig. 7).

MSU1 corresponds to the coarse deposition identified at the base of most of the drill cores (BRD8, BRD9, BRD10, BRD7 and BRG1). It is composed of sands and gravels (GB-Gcm, GB-Gmm, GB-Sm, GB-Sh). This coarse deposition is attributed to an active deposition process such as bedload or the first stage of the deposition of an alluvial plug (Gautier et al., 2007, 2010; Constantine et al., 2010; Toonen et al., 2012; Dieras et al., 2013). According to the CM diagram, fluvial transport modes mainly correspond to rolling and graded suspension (Fig. 7C). A different deposition pattern was evidenced by the core BRD12, which was collected in a chute channel. The base is composed of rhythmic sedimentation with alternating sandy and muddy deposits resulting from an intermittent connection with the main channel during higher discharge events.

MSU2 is characterized by organic bedded silt or massive silty clay, sometime sandy (CH-Fl, CH-Fsm) and interpreted as a fluvio-palustrine environment. The deposit, characteristic of a swampy environment, indicates a cutoff process. Three facies were identified: bedded fine sand and organic silt interpreted as high-energy fluvio-palustrine deposition; bedded organic silt and clay interpreted as low energy fluvio-palustrine deposition, and authigenic deposition such as peat, palustrine carbonate, or diatoms.

The thickness of this layer ranges from 0.07 m (BRD7) to 2.12 m (BRD11). According to the CM diagram, the fluvial transport process corresponds to uniform suspension and settling. Palaeomeanders evolved toward backwater lakes connected to the active channel by the downstream outlet during floods or toward passive lentic lakes flooded by very low-energy flows.

MSU3 corresponds to the upper part of palaeochannel fill. It is made up of a sandy, silty clayey layer (FF-Fsm), whose thickness varies from 0.6 m (BRD10) to 2.25 m (BRD8). According to the CM diagram, the deposition was the result of uniform suspension transport and settling processes. The deposition is attributed to the transition from a lentic to a dried up wetland through sedimentation processes by overbank deposit and biogenetic components.

The assessment of sediment rates concerns the deposition recorded during the fluvio-palustrine phase (MSU2) and the dried-up phase (MSU3) of the evolution of palaeochannels. Their comparison suggests very uneven fill rhythms. In the cores BRD12, BRD9, BRD10 and BRD11, the fill was deposited faster at the beginning of the fluvio-palustrine phase, probably because of the episodic but frequent reconnection with the existing river. In the cores BRD7 and BRD8, the sediment rate is lower at the base of the core and can be interpreted as a permanent disconnection of the palaeochannel after the formation of the alluvial plug.

Four periods with a higher sedimentation rate can be proposed and discussed:

- period 1: between 5272–4867 and 4568–4418 yr cal. BP (base of core BRD9);
- period 2: around 2329–2146 yr cal. BP (core BRD12);
- period 3: between 1522–1346 and 1231–1001 yr cal. BP (bases of cores BRD10 and BRD11);
- period 4: after 780 yr cal. BP (top of cores BRD12, BRD7, BRG1 and BRD8).

The first three periods appear unreliable since they are recorded in only one or two palaeochannels. In addition, the location (distance from the active channel, upstream of downstream hydrological connection with the main channel) and the geometry of the palaeochannel play a key role regarding the degree of abundance of deposited fine sediments (Toonen et al., 2012). However, period 4 corresponds to a higher sediment rate recorded in four palaeomeanders and could be considered as the

signal of a higher fine sediment supply.

Different changes at different time scales were evidenced by cores in the former oxbow lakes in Bigny (Fig. 7A). Indeed, the duration of the transition toward a dried-up wetland, which was estimated using radiocarbon ages, varied considerably. The transition of BRD9 toward a terrestrial environment corresponds to the longest duration recorded (between 3821 and 2753 calibrated years). For BRD7, the duration of the process was difficult to estimate because of the lack of chronological markers, however, it lasted a maximum of 3070–2868 calibrated years. More recent palaeomeanders were converted into a dried-up wetland in one to a few centuries. The BRD12 transition lasted between 392 and 629 calibrated years. The BRD8 and BRD10 transitions correspond to 125–516 calibrated years and 115–521 calibrated years, respectively. The large palaeomeander BRD11 transition process lasted from 114 to 365 calibrated years. The filling of the BRG1 palaeochannel was estimated by proposing a maximum value, because only one chronological marker was available for this sequence. Consequently, the calculation of the duration of the evolution toward a terrestrial environment time included the current period as *terminus ante quem*. The filling was therefore completed in less than 864–998 calibrated years.

4.4. Multiparameter analyses

The BRD12 core (Fig. 8; Table 4) was sampled in a chute channel (Figs. 4 and 5). Compared with the changes in vegetation evidenced in the Loire River valley (Cyprien et al., 2004), low percentages of *Tilia* (lime tree) and *Corylus* (hazelnut) coupled with the dominance of *Quercus* (30-40%) recorded at the base of the core BRD12 are characteristic of the Subatlantic period. Both lime and hazelnut decrease drastically in the pollen record from the Loire River valley around 3600 yr cal. BP. Based on this interpretation, the date of wood remains at 5255 ± 35 BP (*ca* 6000 yr cal. BP; Poz-72130) at the base of the core seems to be older, probably because of reworked sediment processes. Hence, we dated the base between 6000 and 2700 yr cal. BP and most of the deposition appears to have occurred after 2700 yr cal. BP (Iron Age and historical period).

At the onset of the Subatlantic (SU 6), deposition was controlled by fluvial processes. The sandy

inputs indicate that the chute channel was connected to the main channel during flood events. The relative abundance of K, interpreted as a detrital signal, and the highly varying sand content of the deposits suggests hydrological and sedimentary connectivity. It was certainly a high energy environment that functioned as a nonperennial secondary channel (Citterio and Piégay, 2009). The scouring capacity of such a fluvial environment could explain the low sedimentation rate. After 2774–2721 yr cal. BP, the chute channel is progressively converted into a small pond connected less and less frequently as it is shown by the gradual drop in the sand content, probably because of the migration of the main channel and because of the formation of an alluvial plug upstream. It may have functioned as a backwater lake connected with the main channel downstream (Citterio and Piégay, 2009), which mainly trapped allogenic fine sediment and coarse sediment during exceptional floods (SU 5). A palustrine phase (SU 4) around 2315–2145 yr cal. BP probably led to the deposition of authigenic organic sediments (TOC = 3.4–5.9%). An increase in Si/K and in Ca/K ratios is recorded in the deposition of SU 4, supporting the hypothesis that SU 4 is dominated by lacustrine authigenic sedimentation composed of biogenic silica and palustrine carbonates. Such palustrine deposition can be interpreted as the result of complete disconnection from the main river combined with a higher water table. After 2315–2145 yr cal. BP, the transition from a palustrine to a dried-up wetland occurred (SU 3, SU 2 and SU 1) resulting from a drop in the water table or from the definitive silting-up of the wetland. Historical silty deposits highlight a phase of pedogenesis around 1864–1639 yr cal. BP (early Roman Empire) and an increase in Mn content as well as slight variations in sediment content in the size of the sand may denote the precipitation of manganese oxides related to oxygenation processes. A peak in Pb/K around 780–683 yr cal. BP can be interpreted as metal pollution (Elbaz-Poulichet et al., 2011), possibly related to anthropogenic proto-industrial activities in the Middle Ages. According to chronological markers, the transition from a chute channel to a dried-up wetland lasted between 392 and 629 calibrated years.

At the base of the core (SU6-PAZ1), there are indications of human impacts throughout the watershed. Anthropogenic taxa such as *Plantago lanceolata* and *Chenopodiaceae* can be seen from the bottom of the core upwards, mainly indicating livestock grazing, while crops (such as cereals) were still

relatively rare. Nevertheless, forest seems to have been the main land cover. As the deposition of SU 6 denotes allogenic sediment, it is likely that the high percentage of beech is the result of registration at the scale of the upstream catchment. After 2774–2721 yr cal. BP (SU 5-PAZ2), a slight clearance in the landscape affected mainly *Fagus* (beech) and *Ulmus* (elm). The percentages of the riparian forest, especially *Alnus* (alder), also decreased slightly. This slight decrease in forest cover is concomitant with an increase in the percentages of pollen of *Cerealia-type* and *Polygonum aviculare* (fallow plants and/or footpath and ruderal communities) (Behre, 1981). Samples from the SU 4 (PAZ3) suggest an increase in forest cover (mainly elm and beech) and in riparian forest (alder) coupled with a slight decrease in anthropogenic pollens (crops, apophytes and other apophytes) around 2315–2145 yr cal. BP. This phase is followed by maximum forest clearance in the context of increased grazing and agriculture (SU 3-PAZ4). This forest clearance mainly concerned drained areas. The riparian forest experienced little change in the sequence studied.

5. Palaeogeographic reconstructions and discussion

This discussion is organized around the three main points that attest to the originality of our results: (1) the evidence for the persistence of an active meandering pattern since at least *ca* 6000 yr cal. BP until *ca* 950-750 yr. cal. BP, (2) the constitution of a relatively late and weakly developed silty layer in the floodplain during the Late Holocene and (3) the stabilization of the river path since *ca* 950-750 yr. cal. BP.

5.1. Evidence and causes for active meandering processes from *ca* 6000 yr cal. BP until *ca* 950-750 yr. cal. BP

Over the last six millennia, the meandering pattern seems to have been continuous because one to four cutoffs were recorded in every millennium in both study areas (Figs. 10 and 11) and no other fluvial patterns have been recognized. Climate changes recorded during the Holocene (Macklin et al., 2010; Magny, 2004; Mayewski et al., 2004) as well as land-use changes in the catchment area or in the valley bottom (Fig. 11) do not seem to have impacted the dynamics of the Cher River sufficiently to alter the fluvial pattern.

During this period, two cutoffs (BRD9, BRD7) were identified in Bigny before historical times (Fig. 10A and B) and five cutoffs (TRG5, TRG3; TRG1, TRG4, TRD-Ch1) in Thénioux. An aerial survey conducted at Bigny revealed a hemispheric enclosure attributed to the Neolithic or the proto-historical period (Rialland, 1991) located in the valley bottom very close to the riparian area of the BRD9 channel that may have been active in the meantime (Fig. 10A). Several Gallo-Roman archeological remains are evidence for groups of humans living in the floodplain (Gandini, 2006; Holmgren, 1981, 2013). Among them, a *villa* located close to palaeochannels BRD9 and BRD7 was dated between 2000 and 1720 yr cal. BP (Gandini, 2006) (Fig. 10D, E and F). From the Late Gallo-Roman period on, the abandonment of several meanders (BRD8, BRD10, BRD11) were identified in Bigny (Fig. 10D, E and F). According to its location, it is likely that the palaeomeander BRD10 corresponds to a re-excavation of an older abandoned channel rather to the development of a new meander loop growing laterally (Fig. 10C and D). Lateral accretion facies (TRG-LA: 1702–1184 yr cal. BP) coupled with the cutoff of a meander (TRG2: 1543–1409 yr cal. BP) were also identified in Thénioux. Between 1303 and 1184 yr cal. BP, the BRD11 channel was rapidly abandoned and became an oxbow lake (Fig. 10F). Up to 1276–1080 yr cal. BP, the lake filled rapidly partly because of the high rate of accumulation of fluvio-palustrine sedimentation. The lake dried up between 1276–1080 and 1070–938 yr cal. BP (seventh–eleventh centuries cal. AD). The transition to a drier environment was also recorded around 1227–1006 yr cal. BP in the palaeomeander BRD8 and after 1231–1001 yr cal. BP in the palaeomeander BRD10 (Fig. 7A).

Active meandering processes and channel mobility are generally conceptualized as the balance between the resistance of floodplain sediment to lateral erosion and the shear stress exerted by the flow (Charlton, 2007). The resistance of sediment to erosion is mostly determined by grain size that controls the cohesiveness of the bank material, and by the type of proximal riparian vegetation (Charlton, 2007; Fisk, 1947; Güneralp and Rhoads, 2011; Gurnell, 2014; Micheli et al., 2004; Motta et al., 2012; Steiger et al., 2005; Thorne, 1982; Thorne and Tovey, 1981; Thorne, 1990). Our observations show that the Holocene deposition mostly consists of the coarse sediments that composed the main part of the floodplain fill (Figs. 4 and 12). It may have limited the cohesiveness of the

riverbanks and their resistance to the strength of the flow. For the last two centuries, it has been demonstrated that, despite a low available energy, lateral mobility of the river was promoted because of the weak resistance of banks, resulting from their composite structure and the coarseness of their base layer (Dépret et al., 2017b, 2015). This results in a low specific stream power required for lateral erosion to occur (Dépret et al., 2017b, 2015). In addition, because of this high bank erodibility, but also because of the low differential of energy between small and large floods, it has been shown that the lateral activity is mainly controlled by low magnitude hydrological events (Dépret et al., 2015). Such a feature indicates a high potential for a continuously or quasi-continuously maintenance of erosive activity during the whole study period. However, the comparison has to be made with caution as we do not have reliable information on the past flow regime, which may have varied because of changes in the rainfall regime and the enhancement of runoff processes caused by land-use changes (Brisset et al., 2017; Lespez et al., 2007; Macaire et al., 2006) and because our reconstructions are mainly based on discontinuous sedimentary records.

The riparian forest also appears to be a determining factor in bank erosion at the scale of the riverbed. Because riparian forest increases the resistance of river banks (Gurnell, 2014; Steiger et al., 2005; Thorne, 1990), a reduction in stabilizing root systems would have increased channel dynamics (Brown et al., 2018; Micheli et al., 2004). Our knowledge of the history of the riparian forest in the Cher River valley is focused on the proto-historical period and the beginning of the Gallo-Roman period. According to the pollen analyses (Fig. 9), as the percentage of *Alnus* was around 20%, the riparian forest seems to have already been affected by forest clearance since the beginning of the study period. This is consistent with the regional synthesis of the middle and downstream Loire Valley provided by Cyprien et al. (2004) who demonstrated an earlier significant drop in the percentage of *Alnus* since *ca* 3300 yr cal. BP. As this clearance is contemporaneous with an increase in cereals (Cyprien et al., 2004), it is very likely human-forced. Theoretically, clearance of vegetation adjacent to the channel should enhance the shifting of the river. However, further pollen analyses are needed to fully understand how the dynamics of the riparian forest affected the lateral mobility of the river during historical times. Therefore, based on our present knowledge, it is likely that coarse sediments that

composed the main part of the floodplain fill are the main factor explaining the lateral mobility (Fig. 12).

We can propose durations of floodplain turnover and speed of recycling (Table 5) based on the palaeomeanders of Bigny that occupy the entire floodplain. Considering that the existing river is inherited from the eleventh-thirteenth centuries cal. AD (1000-1200 yr cal. AD/ 950-750 yr cal. BP), the distance and the ages of the palaeomeanders BRD7, BRD8, BRD9 and BRD11 help to assess the floodplain turnover duration. BRD10 was excluded because it is considered as a reoccupation of an older abandoned meander. The palaeomeanders BRD7 and BRD9 located on the edge of the floodplain indicates a turnover time of *ca* 2.46-2.82 ka (speed of recycling of the floodplain between 0.25-0.35 m.yr^{-1}) and *ca* 3.92-4.52 ka (speed of recycling of the floodplain between 0.22-0.28 m.yr^{-1}), respectively (Table 5). These durations seem to be noticeably higher than those reported in the literature because the floodplain turnover of northern England rivers corresponds to 0.1-1 ka (Feeney et al., 2020), and the floodplain turnover of the Geul River (The Netherlands) corresponds to 0.2-0.3 ka (Moor et al., 2007). In tropical fluvial systems, Aalto et al. (2008) found a recycling time of *ca* 1 ka for the Strickland River (Papua New Guinea) and Gautier et al. (2007) attributed a turnover time of 0.04-0.4 ka to the very laterally active Beni River (Amazonian Bolivia). Values obtained from the historical palaeomeanders BRD8 and BRD11 are lower because the theoretical durations of floodplain turnover correspond to *ca* 0.61-1.18 ka (speed of recycling of the floodplain between 0.42-1.40 m.yr^{-1}) and *ca* 0.35-0.84 ka (speed of recycling of the floodplain between 1.29-3.06 m.yr^{-1}), respectively. Such differences could result from the combined variability of the bank resistance and of the flood regime, but it could also be the simple effect of the duration of the reference periods. Indeed, Donovan and Belmont (2019) demonstrated from aerial photographs series that the measurement of meander migration rates are time-scale dependent. Moreover, rates of reworking extent are necessarily dependent on the ratio between the width of the riverbed and the width of the floodplain. This parameter is highly variable from one fluvial system to another, it partly explains the variability of the proposed rates.

5.2. Constitution of a silty layer in the valley bottom and its relationship with the

catchment properties (land-use changes and physiographic intrinsic components)

Land-use changes at the scale of the catchment are likely to deliver to the valley bottom abundant supplies of fine sediments because of accelerated soil erosion (Brisset et al., 2017; Charlton, 2007; Lespez et al., 2007; Macaire et al., 2006). A clear increase in sedimentation was recorded in many catchments of temperate Europe synchronized with the onset of the agriculture during the Neolithic or with the intensification of such practices when the early farmers did not significantly influence the rhythms of deposition (Notebaert and Verstraeten, 2010). Climatic events occurring in an environment weakened by farming and grazing practices may also affect sediment rates during this period (Notebaert and Verstraeten, 2010). This explains why massive fine loamy sediment deposition is generally recorded in floodplains in France (Beauchamp et al., 2017a, 2017b; Lespez et al., 2007; Pastre et al., 2002; Morin et al., 2011) and more widely throughout northwestern Europe (e.g., Foulds and Macklin, 2006; Notebaert and Verstraeten, 2010) during the Late Holocene. Theoretically, the constitution of such a layer of fine sediment in the floodplain may have enhanced the cohesiveness of banks and therefore their resistance to the flow strength. In that case, the banks would nevertheless be vertically homogeneous. Indeed, Thorne (1982) and Thorne and Tovey (1981) showed that vertically heterogeneous banks with fine sediments dominating only in the upper layer can be considered as highly erodible.

Palaeoecological studies in the Cher River basin provide evidence for land-use changes since the transition from the Middle to the Late Neolithic. The study of charcoal conducted at Loge-à-Magnard marsh, near Bigny, (Vannière and Martineau, 2005) and Grand Chaumet marsh, near Thénioux, (Vannière and Laggoun-Defarge, 2002) detected early anthropogenic fires from 5050 and 5150 yr cal. BP, respectively (Fig. 11). Pollen analyses of core BRD12 (Fig. 9) provide evidence for land-use changes at least from the proto-historical period. Between the late Iron Age and early Gallo-Roman period, societies cleared the forest land cover and the increase in farming and grazing practices is most likely the cause of this significant clearance process. Forest clearance at the end of the Iron Age is consistent with pollen records from the Middle Loire Valley (Cyprien et al., 2004). By studying charcoal remains conserved in the floodplain of the Cher River at Vierzon (just upstream of the Thénioux site), Vannière (2003) also identified a period of regional forest clearance using fire

characterized by the abundance of small-sized coals around 1696–1148 yr cal. BP (Fig. 11). This intensification of grazing and farming practices is also supported by the large scale study by Gandini (2006) that showed that rural settlements spread and diversified from the late Iron Age on, and reached a peak in the second century cal. AD (Fig. 11).

Based on our dataset, the chronological markers indicate that a silty layer has been formed around the end of the proto-historical period and a higher sedimentation rate is recorded in several palaeochannels after 780 yr cal. BP (Fig. 7). However, the formation of fine deposits is not synchronized with the onset of human land-use changes initiated since the Middle/Late Neolithic (Vannière, 2003; Vannière and Martineau, 2005) but rather with the intensification of the latter since the late Iron Age and early Gallo-Roman period (Fig. 9). This fine sediment layer appears to be relatively weakly developed (0-1.2 m) compared to the total thickness of the floodplain fill (6.2-6.9 m) (Fig. 4). For purposes of comparison, in the Seulles River valley (Normandy, northern France), 60% of Holocene floodplain fill was deposited during the last six centuries and corresponds to silty deposition (Beauchamp et al., 2017a, 2017b). In the Cher River floodplain, the fine sediment layer appears to have been too thin all through the study period to limit the lateral mobility of the river (Fig. 12).

We hypothesize here that physiographic intrinsic components of the catchment may have limited the silty deposition in the valley bottom. First, the gentle gradient of the floodplain as well as the slope at the scale of the catchment may have limited landscape connectivity thereby protecting the valley bottom from abundant silty deposition, or at least increased the delivery time. In addition, sedimentation rates are reported to increase earlier in catchments covered by loess because that kind of sediment is very sensitive for soil erosion (Notebaert and Verstraeten, 2010). The Cher River catchment is located on the southern margin of the part of Europe characterized by a thick cover of Pleistocene loess. In France, deformations related to ice wedges are less widespread below 47°N (Andrieux et al., 2016). The Thénioux and Bigny sites are located on the edge of this area (47.252 and 46.812°N, respectively). Consequently, the thinner covering layer of loess compared with catchments located farther north, e.g., the rivers in Normandy, the Seine, the Somme and the Middle Loire valleys (Antoine et al., 2012, 2003; Beauchamp et al., 2017a, 2017b; Castanet, 2008; Lespez et al., 2007;

Pastre et al., 2003, 2002) may have limited the fine sediment supply and the subsequent aggradation of the valley bottom.

5.3. Causes of the stabilization of the river path since *ca* 950-750 yr. cal. BP

The Little Ice Age (LIA), the major climatic fluctuation of the last millennia, resulted in significant fluvial geomorphic changes, particularly fluvial metamorphosis recorded in several basins in western Europe (Bravard, 1989; Candel et al., 2018; Castanet, 2008; Castanet et al., 2015; Salvador and Berger, 2014; Steinmann, 2015). Thus, we might have expected an increase in lateral activity, with the occurrence of some cutoffs, or even a fluvial metamorphosis on the Cher River.

Yet the fluvial pattern remained unchanged and our dataset indicates that no palaeomeander younger than the eleventh–thirteenth centuries cal. AD was identified in either study area. It contrasts sharply with the previous period for which at least one cutoff per millennium has been dated in the floodplain (Fig. 11). At Bigny, the most recent meander cutoff (BRG1) occurred before 930–796 yr cal. BP (Fig. 10G). After this abandonment, all the palaeochannels studied were definitively dried up or are dry most of the time (Fig. 7A). Oxbow lake environments had disappeared from the floodplain (Fig. 12). Along this reach, the comparison between the oldest known map (Atlas de Trudaine, mid-eighteenth century cal. AD) and the most recent aerial photographs indicates a very similar river course. Therefore, the fluvial system very likely experienced a laterally stable phase during this period (Fig. 12).

It is likely that the many hydraulic structures located in the riverbed are the main explanatory factor for that conspicuous stability. Indeed, such hydraulic engineering works could have hampered lateral migration by preventing sediment transport (because of the introduction of large blocks that exceed the competence of the river in the riverbed, obstruction of main and secondary channels by weirs, dams, and watermills, stabilizing riverbanks nearby the weirs by installing rip-rap, reduction of the discharge because of the by-pass reach).

The early Middle Ages corresponds to the expansion of fluvial hydraulic structures in a wide area of western Europe (Lewin, 2010), mainly watermills (Brown et al., 2018). The Cher River valley is not

an exception because it is host to many engineering structures. One of oldest known hydraulic works was recently found at Bigny. An excavation conducted in the current riverbed evidenced a hydraulic mill dating from the eleventh–thirteenth centuries cal. AD based on wooden piles from 927–736 yr cal. BP (Dumont et al., 2017) (Fig. 10G). A by-pass reach coupled with a dam was also built around 1640 cal. AD. (DDEA du Cher, 2009) (Fig. 10H). The current bankfull specific stream power in the reach under the influence (2 km long) of this dam is around 6.5 $W.m^{-2}$, which is barely higher than the minimum value at which lateral erosion can occur (Dépret et al., 2017b) and much lower than the 26 $W.m^{-2}$ computed for the closest reach that is not influenced by weirs. In Thénioux, at least since the mid-sixteenth century (1563 cal. AD), the equipment of the Rozay sector has been composed of a hydraulic mill called 'moulin de Rozay', a fluvial port called 'Port Péan', and a by-pass-reach for fluvial shipping. A second weir-mill ('Moulin Boutet') associated with a spillway was evidenced downstream and was built in 1495 cal. AD (Franquelin, 1952; Serna, 2013). Currently, the bankfull specific stream power of the section under the direct control of the weir "Moulin Boutet" (5.5 km long) is much lower (0.8 $W.m^{-2}$ on 6 km) than that of the section farther upstream (12.2 $W.m^{-2}$ on 10 km) (Dépret et al., 2017b). Such low specific stream power renders lateral mobility impossible. An increase in the number of weirs led to a very sharp reduction in upstream power over distances that can be significant. Along the 51 km of the Cher River flowing between the Bordes weir and the Preuilly weir, respectively located 2.5 km upstream and 49 km downstream to the Bigny dam, 39% of the river length was under the direct hydraulic influence of weirs (Dépret, 2014). The case of the Bordes mill exemplifies the very ancient presence of such structures in the riverbed. On a 500 m long section of river, Troubat (2014) reports the presence of mill remains of different heights throughout the Middle Ages. The existence of theses mills is attested as early as 1202 cal. AD.

For these reasons, we propose that the planform stability identified after the central Middle Ages at Bigny and Thénioux highlights the prevalence of human forcing on the geomorphic processes by inhibiting lateral migration. Thus, the density and the diversity of engineering works would explain the weak influence of the LIA on the Cher River from the end of the Middle Ages to the end of the nineteenth century cal. AD. This geomorphological functioning, which is closely linked to the

presence of hydraulic structures, still predominates today (Dépret et al., 2017b; 2015). The conspicuous current planform stability is thus hypothesized to be primarily the result of the constraints imposed by the engineering works, and suggests that the Cher River would be able to recover its lateral mobility if they were removed (Dépret et al., 2017b). The absence of cutoffs recorded since the onset of the expansion of fluvial hydraulic structures support this hypothesis and demonstrate that this forcing has affected the lateral dynamics at least since the central Middle Ages.

Conclusion

During the second half of the Holocene (since *ca* 6000 yr cal. BP), meandering channels appear to have been the dominant fluvial pattern in both study areas. This river pattern seems to have lasted several millennia. Nevertheless, regarding meandering processes, we observed two distinct patterns.

We found active meandering processes to persist until the central Middle Ages despite land-use changes at least from the Middle/Late Neolithic. The preservation of such an active geomorphic process is interpreted as the result of the low resistance of the banks to erosion. Indeed, the floodplain fill is mostly composed of coarse material and the fine sediment deposition that occurred later appears to be too limited to inhibit lateral mobility. The characteristic features of the catchment, gentle slopes and the limited fine sediment supply because of the weakly developed Pleistocene loess cover, are suspected to have protected the valley bottom from a significant aggradation even though land-use changes promoted the erosion of slopes.

Human-shaped landscape construction is a nonlinear and complex process consisting of several thresholds. The main tipping point in lateral mobility was reached during the central Middle Ages and the Modern period through the many hydraulic structures located in the riverbed, which caused a drastic decrease in the lateral mobility and inhibited the development of new meander loops. It caused a significant drop in the extent of oxbow lakes. This phenomenon was exacerbated by increased alluviation - although moderate - promoting the filling of ponds located in the former channels. By inhibiting processes such as lateral erosion and hence the morphogenic capacity of the river, the floodplain has lost habitat diversity and current ecological richness.

This case study illustrates how physiographic intrinsic components of the catchment (low resistance of the floodplain to erosion coupled with a weak fine sediment supply) promote active meandering processes and how human practices (densely distributed hydraulic structures in the riverbed) may lead to a significant drop in lateral mobility of meandering systems.

Acknowledgments

This research is associated with the investigation themes of the Zone Atelier Loire, CNRS-INEE (*Centre National de la Recherche Scientifique- Institut Ecologie et Environnement).* It is supported by the AGES-Ancient Geomorphological EvolutionS of the Loire River hydrosystem research program (coordination: Cyril Castanet, 2013–2016) funded by the European Union (FEDER), the *Agence de l'Eau Loire-Bretagne (AELB) and the Etablissement Public Loire* (EPL).

The authors would like to thank the DREAL (*Direction régionale de l'environnement, de l'aménagement et du logement*; Regional Institute of the Environment, Development and Housing) for the provision of the LiDAR DEM, and the BRGM (*Bureau des Recherches Géologiques et Minières*, Mining and Geological Research Institute) and the CEREMA (*Centre d'études et d'expertise sur les risques, l'environnement, la mobilité et l'aménagement*, Centre for Studies and Expertise on Risks, Environment, Mobility and Development) for supplying geological data.

References

Aalto, R., Lauer, J.W., Dietrich, W.E., 2008. Spatial and temporal dynamics of sediment accumulation and exchange along Strickland River floodplains (Papua New Guinea) over decadal-to-centennial timescales. J. Geophys. Res. Earth Surf. 113, 1-22. https://doi.org/10.1029/2006JF000627

Allen, J.R.L., 1965. A Review of the Origin and Characteristics of Recent Alluvial Sediments. Sedimentology 5, 89–191. https://doi.org/10.1111/j.1365-3091.1965.tb01561.x

Andrieux, E., Bertran, P., Saito, K., 2016. Spatial analysis of the French Pleistocene permafrost by a GIS database. Permafr. Periglac Process 27, 17–30. https://doi.org/10.1002/ppp.1856

Antoine, P., Fagnart, J.P., Auguste, P., coudret, P., Limondin-Lozouet, N., Ponel, P., Munaut, A.V., Defgnée, A., Gauthier, A., Fritz, C., 2012. Conty, vallée de la Selle (Somme, France):

séquence tardiglaciaire de référence et occupations préhistoriques. Quaternaire, hors-série n°5, Quaternaire.

Antoine, P., Munaut, A.-V., Limondin-Lozouet, N., Ponel, P., Dupéron, J., Dupéron, M., 2003. Response of the Selle River to climatic modifications during the Lateglacial and Early Holocene (Somme Basin-Northern France). Quat. Sci. Rev., 22, 2061–2076. https://doi.org/10.1016/S0277-3791(03)00180-X

Bajard, M., Sabatier, P., David, F., Develle, A.-L., Reyss, J.-L., Fanget, B., Malet, E., Arnaud, D., Augustin, L., Crouzet, C., Poulenard, J., Arnaud, F., 2016. Erosion record in Lake La Thuile sediments (Prealps, France): Evidence of montane landscape dynamics throughout the Holocene. The Holocene 26, 350–364. https://doi.org/10.1177/0959683615609750

Beauchamp, A., Lespez, L., Delahaye, D., 2017a. Impacts des aménagements hydrauliques sur les systèmes fluviaux bas-normands depuis 2000 ans, premiers résultats d'une approche géomorphologique et géoarchéologique dans la moyenne vallée de la Seulles. Quaternaire, 28, 2, 253–258. https://doi.org/10.4000/quaternaire.8153

Beauchamp, A., Lespez, L., Rollet, A.-J., Germain-Vallée, C., Delahaye, D., 2017b. Les transformations anthropiques d'un cours d'eau de faible énergie et leurs conséquences, approche géomorphologique et géoarchéologique dans la moyenne vallée de la Seulles, Normandie. Géomorphologie Relief Process. Environ. 23, 2, 121-138, https://doi.org/10.4000/geomorphologie.11702

Behre, K.E., 1981. interpretation of anthropogenic indicators in pollen diagrams. Pollen Spores 23, 225–245.

Blott, S.J., Pye, K., 2001. GRADISTAT: a grain size distribution and statistics package for the analysis of unconsolidated sediments. Earth Surf. Process. Landf. 26, 1237–1248. https://doi.org/10.1002/esp.261

Bravard, J.-P., 1989. La métamorphose des rivières des Alpes françaises à la fin du Moyen Age et à l'Epoque Moderne. Bull. Société Géographique Liège, 25, 145–157.

Brisset, E., Guiter, F., Miramont, C., Delhon, C., Arnaud, F., Disnar, J.-R., Poulenard, J., Anthony, E., Meunier, J.-D., Wilhelm, B., Pailles, C., 2012. Approche multidisciplinaire d'une séquence lacustre holocène dans les alpes du sud au Lac Petit (Mercantour, alt. 2 200 m, France) : histoire d'un géosystème dégradé. Quaternaire, 23, 4, 309-319, https://doi.org/10.4000/quaternaire.6390

Brisset, E., Guiter, F., Miramont, C., Toussier, T., Sabatier, P., Poher, Y., Cartier, R., Arnaud, F., Malet, E., Anthony, E.J., 2017. The overlooked human influence in historic and prehistoric floods in the European Alps. Geology 45, 347–350. https://doi.org/10.1130/G38498.1

Bronk Ramsey, C., 2009. Bayesian Analysis of Radiocarbon Dates. Radiocarbon 51, 337–360. https://doi.org/10.1017/S0033822200033865

Brooks, G., 2003. Holocene lateral channel migration and incision of the Red River, Manitoba, Canada. Geomorphology 54, 197–215. https://doi.org/10.1016/S0169-555X(02)00356-2

Brown, A., Toms, P., Carey, C., Rhodes, E., 2013. Geomorphology of the Anthropocene: Time-transgressive discontinuities of human-induced alluviation. Anthropocene 1, 3–13. https://doi.org/10.1016/j.ancene.2013.06.002

Brown, A.G., Lespez, L., Sear, D.A., Macaire, J.-J., Houben, P., Klimek, K., Brazier, R.E., Van Oost, K., Pears, B., 2018. Natural vs anthropogenic streams in Europe: History, ecology and implications for restoration, river-rewilding and riverine ecosystem services. Earth-Sci. Rev. 180, 185–205. https://doi.org/10.1016/j.earscirev.2018.02.001

Bunte, K., Abt, S.R., 2001. Sampling Surface and Subsurface Particle-Size Distributions in Wadable Gravel- and Cobble-Bed Streams for Analyses in Sediment Transport, Hydraulics, and Streambed Monitoring. United States Department of Agriculture, Rocky Mountain Research Station, Fort Collins.

Candel, J.H.J., Kleinhans, M.G., Makaske, B., Hoek, W.Z., Quik, C., Wallinga, J., 2018. Late Holocene channel pattern change from laterally stable to meandering caused by climate and land use changes. Earth Surf. Dyn. 6, 723–741, https://doi.org/10.5194/esurf-2018-31

Carcaud, N., 2004. D'espace et de temps : un itinéraire de recherche et d'enseignement sur les anthroposystème fluviaux, (HDR thesis) ed. Université d'Angers.

Castanet, C., 2008. La Loire en val d'Orléans: dynamiques fluviales et socio-environnementales

durant les derniers 30 000 ans : de l'hydrosystème à l'anthroposystème (PhD thesis). Université Panthéon-Sorbonne, Paris, France.

Castanet, C., Burnouf, J., Camerlynck, C., Carcaud, N., Cyprien-Chouin, A.-L., Garcin, M., Lamothe, M., 2015. Holocene fluvial dynamic of the middle Loire River (Val d'Orléans, France): responses to climatic variability and anthropogenic impacts, in: French Geoarchaeology in the 21st Century (Dir. Arnaud-Fassetta G. and Carcaud N), ed. CNRS, 119–130.

Charlton, R., 2007. Fundamentals of Fluvial Geomorphology, 1st ed. Routledge, London ; New York.

Citterio, A., Piégay, H., 2009. Overbank sedimentation rates in former channel lakes: characterization and control factors. Sedimentology 56, 461–482. https://doi.org/10.1111/j.1365-3091.2008.00979.x

Citterio, A., Piégay, H., 2000. L'atterrissement des bras morts de la basse vallée de l'Ain : dynamique récente et facteurs de contrôle. Géomorphologie Relief Process. Environ. 6, 87–104. https://doi.org/10.3406/morfo.2000.1050

Constantine, J.A., Dunne, T., PiéGay, H., Mathias Kondolf, G., 2010. Controls on the alluviation of oxbow lakes by bed-material load along the Sacramento River, California. Sedimentology 57, 389–407. https://doi.org/10.1111/j.1365-3091.2009.01084.x

Cossalter, F., 2011. Des carrières alluviales aux captures dans la vallée du Cher, analyses spatiales et méthode de mesures des impacts hydrologiques et sédimentaires (Master thesis). Université Paris 1 Panthéon-Sorbonne, Paris.

Cyprien, A.-L., Visset, L., Carcaud, N., 2004. Evolution of vegetation landscapes during the Holocene in the central and downstream Loire basin (Western France). Veget Hist Archaeobot 13, 181–196. https://doi.org/10.1007/s00334-004-0042-y

DDEA du Cher, 2009. Arasement du barrage de Bigny sur le Cher commune de VALLENAY (18), rapport de phase 1, etude hydraulique et morphodynamique.

Dépret, T., 2014. Fonctionnement morphodynamique actuel et historique des méandres du Cher. (PhD thesis). Université Paris 1 Panthéon-Sorbonne, Paris.

Dépret, T., Riquier, J., Piégay, H., 2017a. Evolution of abandoned channels: Insights on controlling factors in a multi-pressure river system. Geomorphology, 294, 99–118. https://doi.org/10.1016/j.geomorph.2017.01.036

Dépret, T., Gautier, E., Hooke, J., Grancher, D., Virmoux, C., Brunstein, D., 2017b. Causes of planform stability of a low-energy meandering gravel-bed river (Cher River, France). Geomorphology, 285, 58–81. https://doi.org/10.1016/j.geomorph.2017.01.035

Dépret, T., Gautier, E., Hooke, J., Grancher, D., Virmoux, C., Brunstein, D., 2015. Hydrological controls on the morphogenesis of low-energy meanders (Cher River, France). J. Hydrol. 531, 877–891. https://doi.org/10.1016/j.jhydrol.2015.10.035

Dieras, P.L., 2013. The persistence of oxbow lakes as aquatic habitats: An assessment of rates of change and patterns of alluviation (PhD thesis). Cardiff University.

Dieras, P.L., Constantine, J.A., Hales, T.C., Piégay, H., Riquier, J., 2013. The role of oxbow lakes in the off-channel storage of bed material along the Ain River, France. Geomorphology 188, 110–119. https://doi.org/10.1016/j.geomorph.2012.12.024

Donovan, M., Belmont, P., 2019. Timescale dependence in river channel migration measurements. Earth Surf. Process. Landf. 44, 1530–1541. https://doi.org/10.1002/esp.4590

Dumont, A., Moyat, P., Letuppe, J., Lavier, P., Defaix, P., 2017. Le moulin médiéval de Vallenay sur le Cher. SRA.

Ejarque, A., Beauger, A., Miras, Y., Peiry, J.-L., Voldoire, O., Vautier, F., Benbakkar, M., Steiger, J., 2014. Historical fluvial palaeodynamics and multi-proxy palaeoenvironmental analyses of a palaeochannel, Allier River, France. Geodin. Acta, 27, 1, 25-47, DOI: 10.1080/09853111.2013.877232.

Elbaz-Poulichet, F., Dezileau, L., Freydier, R., Cossa, D., Sabatier, P., 2011. A 3500-year record of Hg and Pb contamination in a mediterranean sedimentary archive (the Pierre Blanche Lagoon, France). Environ. Sci. Technol. 45, 8642–8647. https://doi.org/10.1021/es2004599

Erkens, G., Dambeck, R., Volleberg, K.P., Bouman, M.T.I.J., Bos, J.A.A., Cohen, K.M., Wallinga, J., Hoek, W.Z., 2009. Fluvial terrace formation in the northern Upper Rhine Graben during the last 20000 years as a result of allogenic controls and autogenic evolution. Geomorphology 103, 476–495. https://doi.org/10.1016/j.geomorph.2008.07.021

Erskine, W., McFadden, C., Bishop, P., 1992. Alluvial cutoffs as indicators of former channel conditions. Earth Surf. Process. Landf. 17, 23–37. https://doi.org/10.1002/esp.3290170103

Faegri, K., Iversen, J., Kaland, P.E., 2000. Textbook of Pollen Analysis, 4th Edition edition. ed. The Blackburn Press, Caldwell, NJ.

Feeney, C.J., Chiverrell, R.C., Smith, H.G., Hooke, J.M., Cooper, J.R., 2020. Modelling the decadal dynamics of reach-scale river channel evolution and floodplain turnover in CAESAR-Lisflood. Earth Surf. Process. Landf. 45, 1273–1291. https://doi.org/10.1002/esp.4804

Fisk, H.N., 1947. Fine-grained alluvial deposits and their effects on Mississippi River activity. Miss. River Comm. vols. 1 & 2, 82.

Foulds, S.A., Macklin, M.G., 2006. Holocene land-use change and its impact on river basin dynamics in Great Britain and Ireland. Prog. Phys. Geogr. Earth Environ. 30, 589–604. https://doi.org/10.1177/0309133306071143

Franquelin, C., 1998. Evolutions diachroniques des formes et de la dynamiques du Cher entre Vierzon et Saint-Aignan (Master thesis). Université de Tours.

Gandini, C., 2008. Des campagnes gauloises aux campagnes de l'Antiquite tardive. La dynamique de l'habitat rural dans la cité des Bituriges Cubi (IIe s av JC - VIIe ap. JC.), Revue archéologique du Centre de la France. ed, Supplément à la RACF n°33. Tours.

Gandini, C., 2006. Des campagnes gauloises aux campagnes de l'Antiquité tardive : la dynamique de l'habitat rural dans la cité des Bituriges Cubi (IIe s. av. J.-C. - VIIe s. ap. J.-C.). (PhD thesis). Université Panthéon-Sorbonne - Paris I.

Gautier, E., Brunstein, D., Vauchel, P., Jouanneau, J.-M., Roulet, M., Garcia, C., Guyot, J.-L., Castro, M., 2010. Channel and floodplain sediment dynamics in a reach of the tropical meandering Rio Beni (Bolivian Amazonia). Earth Surf. Process. Landf. 35, 1838–1853. https://doi.org/10.1002/esp.2065

Gautier, E., Brunstein, D., Vauchel, P., Roulet, M., Fuertes, O., Guyot, J.L., Darozzes, J., Bourrel, L., 2007. Temporal relations between meander deformation, water discharge and sediment fluxes in the floodplain of the Rio Beni (Bolivian Amazonia). Earth Surf. Process. Landf. 32, 230–248. https://doi.org/10.1002/esp.1394

Gottesfeld, A.S., Johnson Gottesfeld, L.M., 1990. Floodplain dynamics of a wandering river, dendrochronology of the Morice River, British Columbia, Canada. Geomorphology 3, 159–179. https://doi.org/10.1016/0169-555X(90)90043-P

Güneralp, İ., Rhoads, B.L., 2011. Influence of floodplain erosional heterogeneity on planform complexity of meandering rivers. Geophys. Res. Lett. 38. https://doi.org/10.1029/2011GL048134

Gurnell, A., 2014. Plants as river system engineers. Earth Surf. Process. Landf. 39, 4–25. https://doi.org/10.1002/esp.3397

Hoffmann, T., Erkens, G., Gerlach, R., Klostermann, J., Lang, A., 2009. Trends and controls of Holocene floodplain sedimentation in the Rhine catchment. CATENA, 77, 96–106. https://doi.org/10.1016/j.catena.2008.09.002

Hohensinner, S., Habersack, H., Jungwirth, M., Zauner, G., 2004. Reconstruction of the characteristics of a natural alluvial river–floodplain system and hydromorphological changes following human modifications: the Danube River (1812–1991). River Res. Appl. 20, 25–41.

Holmgren, J., 2013. Prospection aérienne : fermes et villae gallo-romaines du Berry -1. Cah. Archéologie Hist. Berry 3–198.

Holmgren, J., 1981. Prospections aérienne en Berry - III-la région de Saint-Loup-des-Chaumes. Cah. Archéologie Hist. Berry 45–62.

Hooke, J.M., 1995. River channel adjustment to meander cutoffs on the River Bollin and River Dane, northwest England. Geomorphology 14, 235–253. https://doi.org/10.1016/0169-555X(95)00110-Q

Hooke, J.M., 1987. Changes in meander morphology. Int. Geomorphol. 1986 Proc 1st Conf. Vol 1 591–609.

Houben, P., 2003. Spatio-temporally variable response of fluvial systems to Late Pleistocene climate change: a case study from central Germany. Quat. Sci. Rev., 22, 2125–2140. https://doi.org/10.1016/S0277-3791(03)00181-1

Juggins, S., 2017. rioja: Analysis of Quaternary Science Data, R package version (0.9-21).

Konert, M., Vandenberghe, J., 1997. Comparison of laser grain size analysis with pipette and sieve analysis: a solution for the underestimation of the clay fraction. Sedimentology 44, 523–535. https://doi.org/10.1046/j.1365-3091.1997.d01-38.x

Kozarski, S., Rotnicki, K., 1977. Valley floors and changes of river channel patterns in the north Polish Plain during the Late-Wurm and Holocene. Quaest. Geogr. 4, 51–93.

Lablanche, G., Desprez, N., 1984. Carte géologique et notice explicative de la feuille Châteauneuf-sur-Cher au 1/50 000. BRGM, Orléans.

Lablanche, G., Marchand, D., Lefavrais-Raymond, A., Deprand-Passard, S., Gros, Y., Debéglia, N., Maget, P., Lallier, D., 1994. Carte géologique et notice explicative de la feuille Saint-Amand-Montrond au 1/50 000. BRGM, Orléans.

Lespez, L., Clet-Pellerin, M., Limondin-Lozouet, N., Pastre, J.F., Fontugne, M., Marcigny, C., 2007. Fluvial system evolution and environmental changes during the Holocene in the Mue valley (Western France). Geomorphology 98, 55–70. https://doi.org/10.1016/j.geomorph.2007.02.029

Lespez, L., Viel, V., Rollet, A.-J., Delayaye, D., 2015. The anthropogenic nature of present-day low energy rivers in western France and implications for current restoration projects. Geomorphology 251, 64–76. https://doi.org/10.1016/j.geomorph.2015.05.015

Lewin, J., 2010. Medieval environmental impacts and feedbacks: The lowland floodplains of England and Wales. Geoarchaeology 25, 267–311. https://doi.org/10.1002/gea.20308

Lewin, J., Macklin, M.G., 2010. Floodplain catastrophes in the UK Holocene: messages for managing climate change. Hydrol. Process. 24, 2900–2911. https://doi.org/10.1002/hyp.7704

Loke, M.-H., 2000. Electrical imaging surveys forenvironmental and engineering studies, A practical guide to 2-D and 3-D surveys.

Macaire, J.-J., Bernard, J., Di-Giovanni, C., Hinschberger, F., Limondin-Lozouet, N., Visset, L., 2006. Quantification and regulation of organic and mineral sedimentation in a late-Holocene floodplain as a result of climatic and human impacts (Taligny marsh, Parisian Basin, France). The Holocene 16, 647–660. https://doi.org/10.1191/0959683606hl961rp

Macklin, M.G., Jones, A.F., Lewin, J., 2010. River response to rapid Holocene environmental change: evidence and explanation in British catchments. Quat. Sci. Rev. 29, 1555–1576. https://doi.org/10.1016/j.quascirev.2009.06.010

Magny, M., 2004. Holocene climate variability as reflected by mid-European lake-level fluctuations and its probable impact on prehistoric human settlements. Quat. Int. 113, 65–79. https://doi.org/10.1016/S1040-6182(03)00080-6

Manivit, J., Debrand-Passard, S., Gros, Y., Desprez, N., 1994. Carte géologique et notice explicative de la feuille Vierzon au 1/50 000. BRGM, Orléans.

Marescot, L., 2006. Introduction à l'imagerie électrique du sous-sol. Bull. Société Vaudoise Sci. Nat. 90, 23–40.

Mayewski, P.A., Rohling, E.E., Curt Stager, J., Karlén, W., Maasch, K.A., Meeker, L.D., Meyerson, E.A., Gasse, F., van Kreveld, S., Holmgren, K., Lee-Thorp, J., Rosqvist, G., Rack, F., Staubwasser, M., Schneider, R.R., Steig, E.J., 2004. Holocene Climate Variability. Quat. Res. 62, 243–255. https://doi.org/10.1016/j.yqres.2004.07.001

Miall, A.D., 1996. The Geology of Fluvial Deposits: Sedimentary Facies, Basin Analysis, and Petroleum Geology, 1st ed. 1996. Corr. 3rd printing 2006. ed. Springer-Verlag Berlin and Heidelberg GmbH & Co. K, Berlin ; New York.

Micheli, E.R., Kirchner, J.W., Larsen, E.W., 2004. Quantifying the effect of riparian forest versus agricultural vegetation on river meander migration rates, central Sacramento River, California, USA. River Res. Appl. 20, 537–548. https://doi.org/10.1002/rra.756

Mol, J., Vandenberghe, J., Kasse, C., 2000. River response to variations of periglacial climate in mid-latitude Europe. Geomorphology 33, 131–148. https://doi.org/10.1016/S0169-555X(99)00126-9

Moor, J.J.W. Balen, R.T. Kasse, C., 2007. Simulating meander evolution of the Geul River (the Netherlands) using a topographic steering model. Earth Surf. Process. Landf. 32, 1077–1093. https://doi.org/10.1002/esp.1466

Moore, P.D., 1991. Pollen analysis, 2nd ed. ed. Blackwell Science, Oxford, Malden, MA.

Morin, E., Macaire, J.-J., Hinschberger, F., Gay-Ovéjéro, I., Rodrigues, S., Bakyono, J.-P., Visset, L.,

2011. Spatio-temporal evolution of the Choisille River (southern Parisian Basin, France) during the Weichselian and the Holocene as a record of climate trend and human activity in north-western Europe. Quat. Sci. Rev. 30, 347–363. https://doi.org/10.1016/j.quascirev.2010.11.015

Motta, D., Abad, J.D., Langendoen, E.J., García, M.H., 2012. The effects of floodplain soil heterogeneity on meander planform shape. Water Resour. Res. 48. 1-17 https://doi.org/10.1029/2011WR011601

Murray, A.S., Olley, J.M., 2002. Precision and accuracy in the optically stimulated luminescence dating of sedimentary quartz: a status review. Geochronometria Vol. 21, 1–16.

Murray, A.S., Wintle, A.G., 2000. Luminescence dating of quartz using an improved single-aliquot regenerative-dose protocol. Radiat. Meas. 32, 57–73. https://doi.org/10.1016/S1350-4487(99)00253-X

Notebaert, B., Broothaerts, N., Verstraeten, G., 2018. Evidence of anthropogenic tipping points in fluvial dynamics in Europe. Glob. Planet. Change 164, 27–38. https://doi.org/10.1016/j.gloplacha.2018.02.008

Notebaert, B., Verstraeten, G., 2010. Sensitivity of West and Central European river systems to environmental changes during the Holocene: A review. Earth-Sci. Rev. 103, 163–182. https://doi.org/10.1016/j.earscirev.2010.09.009

Notebaert, B., Verstraeten, G., Govers, G., Poesen, J., 2009. Qualitative and quantitative applications of LiDAR imagery in fluvial geomorphology. Earth Surf. Process. Landf. 34, 217–231. https://doi.org/10.1002/esp.1705

Passega, R., 1957. Textures as characteristic of clastic deposition. Am. Assoc. Pet. Geol. Bull. 9, 1952–1984.

Pastre, J.-F., Leroyer, C., Limondin-Lozouet, N., Fontugne, M., Hatté, C., Krier, V., Kunesch, S., Saad, M.-C., 2002. L'Holocène du bassin parisien : variation environnementale et réponses géoécologiques des fonds de vallée, in: Equilibres et Rupture Dans Les Écosystèmes Depuis 20000 Ans En Europe de l'Ouest - Actes Du Colloque International de Besançon 18-22 Septembre 2000 (Dir. Richard H. ; Vigot A.), ed. Presses universitaires de Franche-Comté, 61–73.

Pastre, J.-F., Limondin-Lozouet, N., Leroyer, C., Ponel, P., Fontugne, M., 2003. River system evolution and environmental changes during the Lateglacial in the Paris Basin (France). Quat. Sci. Rev. 22, 2177–2188. https://doi.org/10.1016/S0277-3791(03)00147-1

Petts, G.E., Amoros, C., 1996. Fluvial Hydrosystems, ed. Chapman and Hall, London ; New York.

Prescott, J.R., Hutton, J.T., 1994. Cosmic ray contributions to dose rates for luminescence and ESR dating: Large depths and long-term time variations. Radiat. Meas. 23, 497–500. https://doi.org/10.1016/1350-4487(94)90086-8

R Core Team, 2018. R: A Language and Environment for Statistical Computing. R Foundation for Statistical Computing. Vienna.

Reille, M., 1999. Pollen et spores d'Europe et d'Afrique du Nord. ed. Laboratoire de Botanique Historique et Palynologie, Marseille.

Reimer, P.J., Bard, E., Bayliss, A., Beck, J.W., Blackwell, P.G., Ramsey, C.B., Buck, C.E., Cheng, H., Edwards, R.L., Friedrich, M., Grootes, P.M., Guilderson, T.P., Haflidason, H., Hajdas, I., Hatté, C., Heaton, T.J., Hoffmann, D.L., Hogg, A.G., Hughen, K.A., Kaiser, K.F., Kromer, B., Manning, S.W., Niu, M., Reimer, R.W., Richards, D.A., Scott, E.M., Southon, J.R., Staff, R.A., Turney, C.S.M., van der Plicht, J., 2013. IntCal13 and Marine13 Radiocarbon Age Calibration Curves 0–50,000 Years cal BP. Radiocarbon 55, 1869–1887. https://doi.org/10.2458/azu_js_rc.55.16947

Rialland, Y., 1991. Reconnaissance des enceintes de vallée et de camps de hauteur néolithiques de la vallée du Cher dans le département du Cher -Rapport de prospection thématique pour 1990. Service Régional de l'Archéologie -Région Centre-Val de Loire.

Sabatier, P., Wilhelm, B., Ficetola, G.F., Moiroux, F., Poulenard, J., Develle, A.-L., Bichet, A., Chen, W., Pignol, C., Reyss, J.-L., Gielly, L., Bajard, M., Perrette, Y., Malet, E., Taberlet, P., Arnaud, F., 2017. 6-kyr record of flood frequency and intensity in the western Mediterranean Alps – Interplay of solar and temperature forcing. Quat. Sci. Rev. 170, 121–135. https://doi.org/10.1016/j.quascirev.2017.06.019

Salvador, P.-G., 2005. Géomorphologie et géoarchéologie des plaines alluviales (piémont alpin et nord de la France) (HDR thesis). Université des Sciences et Technologies de Lille, Lille.

Salvador, P.-G., Berger, J., Gauthier, E., Vannière, B., 2004. Holocene fluctuations of the Rhône river in the alluvial plain of the Basses Terres (Isère, Ain, France). Quaternaire 15, 177–186. https://doi.org/10.3406/quate.2004.1765

Salvador, P.-G., Berger, J.-F., 2014. The evolution of the Rhone River in the Basses Terres basin during the Holocene (Alpine foothills, France). Geomorphology 204, 71–85. https://doi.org/10.1016/j.geomorph.2013.07.030

Serna, V., 2013. Le Cher. Histoire et archéologie d'un cours d'eau. Revue archéologique du Centre de la France - Suppléments, Tours.

Service Régional de l'Archéologie-Centre Val de Loire, 2017. Base de données PATRIARCHE.

Steiger, J., Tabacchi, E., Dufour, S., Corenblit, D., Peiry, J.-L., 2005. Hydrogeomorphic processes affecting riparian habitat within alluvial channel–floodplain river systems: a review for the temperate zone. River Res Applic 21, 719–737. https://doi.org/10.1002/rra.879

Steinmann, R., 2015. L'influence climatique et anthropique sur trois cours d'eaux bourguignons : géoarchéologie de sites de franchissement sur la Loire, la Saône et le Doubs au cours de l'Holocène (PhD thesis). Université de Bourgogne.

Steinmann, R., Garcia, J.-P., Dumont, A., Quiquerez, A., 2017. Aspects méthodologiques de l'approche intégrée des comblements postglaciaires : apports pour la reconstitution de la dynamique fluviale de la Loire au cours de l'Holocène. Géomorphologie Relief Process. Environ. 23, 83–104. https://doi.org/10.4000/geomorphologie.11650

Stølum, H.-H., 1996. River Meandering as a Self-Organization Process. Science 271, 1710–1713. https://doi.org/10.1126/science.271.5256.1710

Thorne, C. R., 1990. Effects of vegetation on riverbank erosion and stability, in: Vegetation and Erosion: Processes and Environments (Dir. Thornes J. B), ed. John Wiley & Sons, Chichester, 125–144.

Thorne, C.R., 1982. Processes and mechanisms of river bank erosion, in: Hey, R.D., Bathurst, J.C., Thorne, C.R. (Eds.), Gravel-Bed Rivers: Fluvial Processes, Engineering and Management. ed. John Wiley & Sons, Chichester, 227–271.

Thorne, C.R., Tovey, N.K., 1981. Stability of composite river banks. Earth Surf. Process. Landf. 6, 469–484. https://doi.org/10.1002/esp.3290060507

Toonen, W.H.J., Kleinhans, M.G., Cohen, K.M., 2012. Sedimentary architecture of abandoned channel fills. Earth Surf Process Landf. 37, 459–472. https://doi.org/10.1002/esp.3189

Troubat, O., 2014. Bruère-Allichamps/Vallenay (Cher). Allichamps. Archéologie Médiév. 184–185.

Udden, J.-A., 1914. Mechanical composition of clastic sediments. Bull. Geol. Soc. Am. 25, 655–744.

Vandenberghe, J., 2008. The fluvial cycle at cold–warm–cold transitions in lowland regions: A refinement of theory. Geomorphology, 98, 275–284. https://doi.org/10.1016/j.geomorph.2006.12.030

Vandenberghe, J., 2003. Climate forcing of fluvial system development: an evolution of ideas. Quat. Sci. Rev., Fluvial response to rapid environmental change 22, 2053–2060. https://doi.org/10.1016/S0277-3791(03)00213-0

Vandenberghe, J., 1993. Changing fluvial processes under changing periglacial conditions. Z. Für Geomorphol. 17–28.

Vandenberghe, J., Kasse C., Bohncke S., Kozarski S., 1994. Climate-related river activity at the Weichselian-Holocene transition: a comparative study of the Warta and Maas rivers. Terra Nova 6, 476–485. https://doi.org/10.1111/j.1365-3121.1994.tb00891.x

Vannière, B., 2003. Les micro-charbons: indicateur paléoenvironnemental de l'anthropisation. Exemple d'étude en contexte alluvial (Vierzon, Cher), in: Actualité de la recherche en histoire et archéologie agraires: actes du colloque AGER V, 19-20 septembre 2000. ed. Presses Universitaires de Franche-Comté, 283–296.

Vannière, B., Laggoun-Defarge, F., 2002. Première contribution à l'étude des évolutions paléohydrologiques et à l'histoire des feux en Champagne berrichonne durant l'Holocène. Le cas du "Marais du Grand-Chaumet" (Indre, France), in: Les Fleuves Ont Une Histoire, Paléo-Environnement Des Rivières et Des Lacs Français Depuis 15 000 Ans, (Dir. Bravard J-P. et Magny M.), ed. Errance 101–124.

Vannière, B., Martineau, R., 2005. Histoire des feux et pratiques agraires du Néolithique à l'âge du Fer en région Centre : implications territoriales, démographiques et environnementales. Gall. Préhistoire 47, 167–186. https://doi.org/10.3406/galip.2005.2049

Vayssière, A., 2018. Trajectoires et processus fluviaux dans la moyenne vallée du Cher du Tardiglaciaire à la période actuelle. Métamorphose fluviale, réponses aux forçages sociétaux et ajustements des chenaux et des bras morts (PhD thesis). Université Paris 1 Panthéon-Sorbonne, Paris.

Vayssière, A., Depret, T., Castanet, C., Gautier, E., Virmoux, C., Carcaud, N., Garnier, A., Brunstein, D., Pinheiro, D., 2016. Etude des paléoméandres holocènes de la plaine alluviale du Cher (site de Bigny, moyenne vallée du Cher). Géomorphologie Relief Process. Environ. 22, 163–176. https://doi.org/10.4000/geomorphologie.11369

Vayssière, A., Rué, M., Recq, C., Gardère, P., Bozsó, E., Castanet, C., Virmoux, C., Gautier, E., 2019. Lateglacial changes in river morphologies of northwestern Europe: An example of a smooth response to climate forcing (Cher River, France). Geomorphology, 342, 20-36 https://doi.org/10.1016/j.geomorph.2019.05.019

Visset, L., Cyprien, A.L., Carcaud, N., Bernard, J., Ouguerram, A., 2005. Paysage végétal dans le bassin de la Loire moyenne du Tardiglaciaire à l'Actuel. J. Bot. Société Bot. Fr. 29, 41–51.

Wentworth, C.K., 1922. A scale of grade and class terms for clastic sediments. J. Geol. 30, 377–392.

Figures list

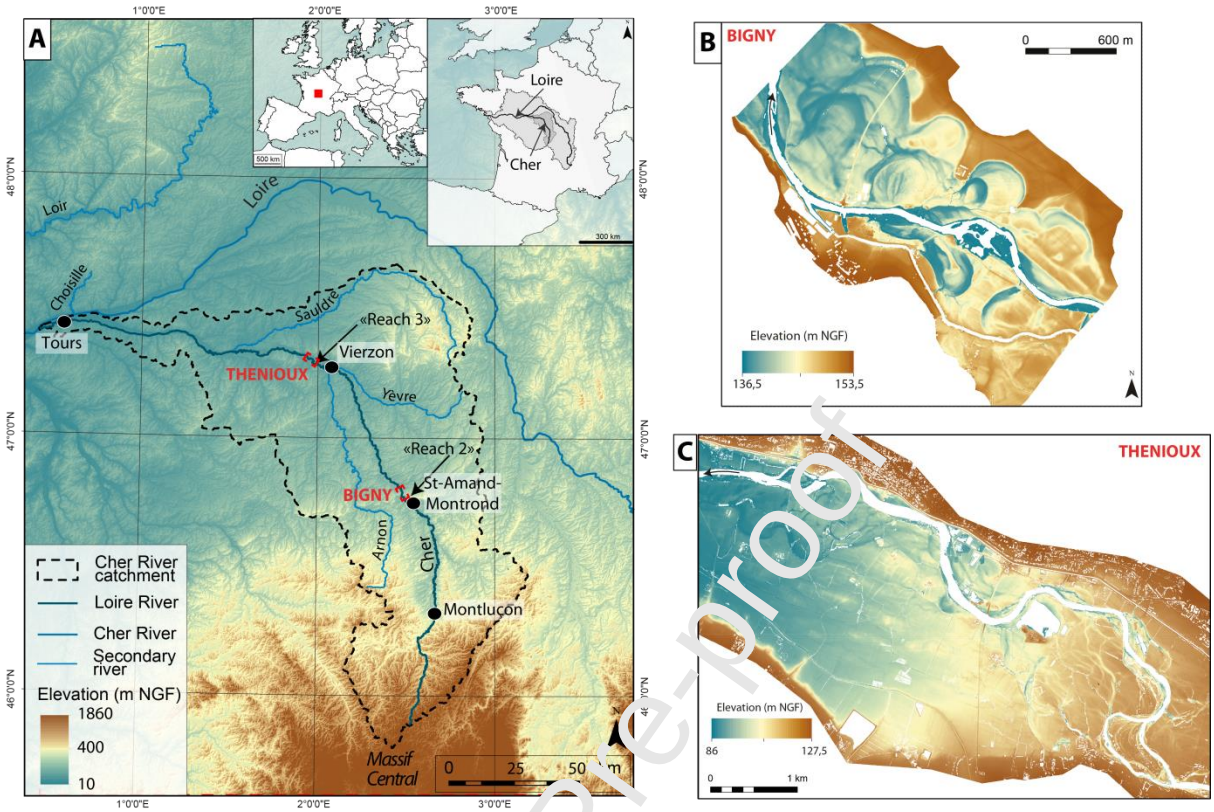

Fig. 1. A. Topographical map of the Cher River basin. B. LiDAR DEM of the Bigny site. C. LiDAR DEM of the Thénioux site.

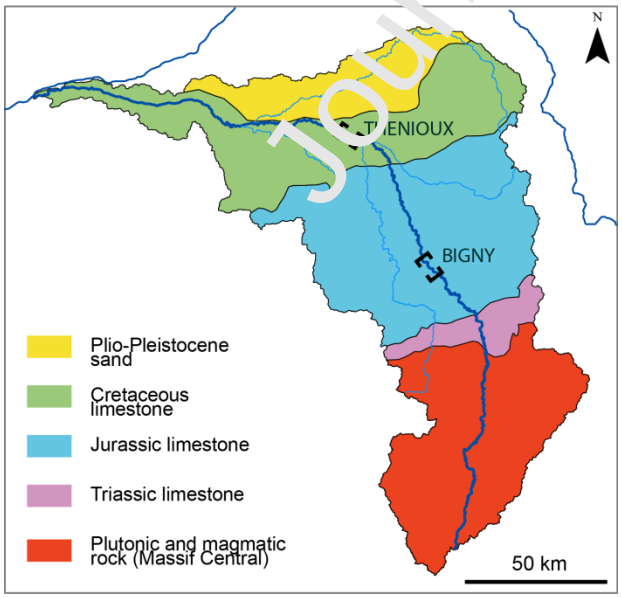

Fig. 2. Main geological units of the Cher River catchment

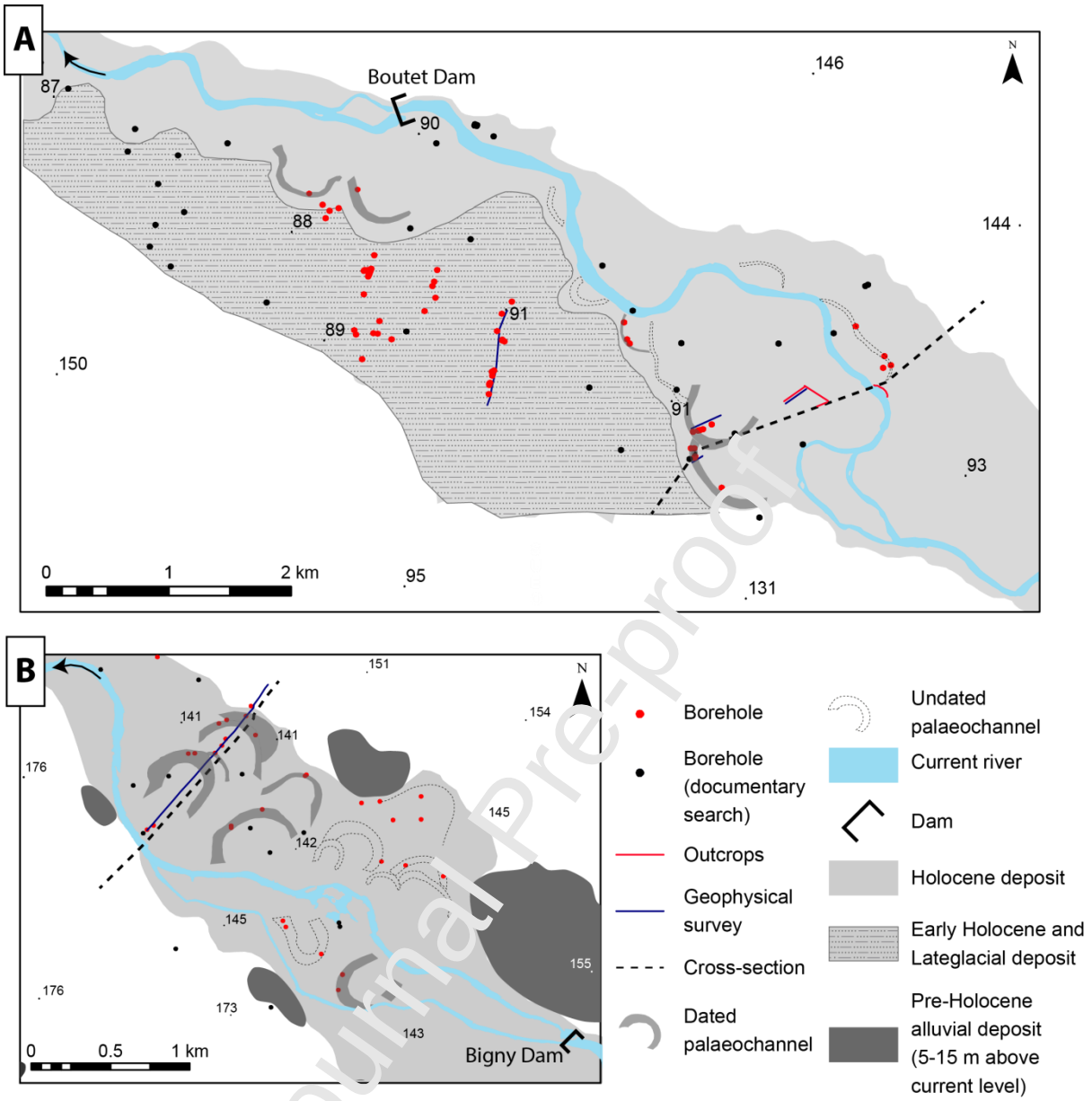

Fig. 3. Field survey strateg . A. Thénioux reach; B. Bigny reach

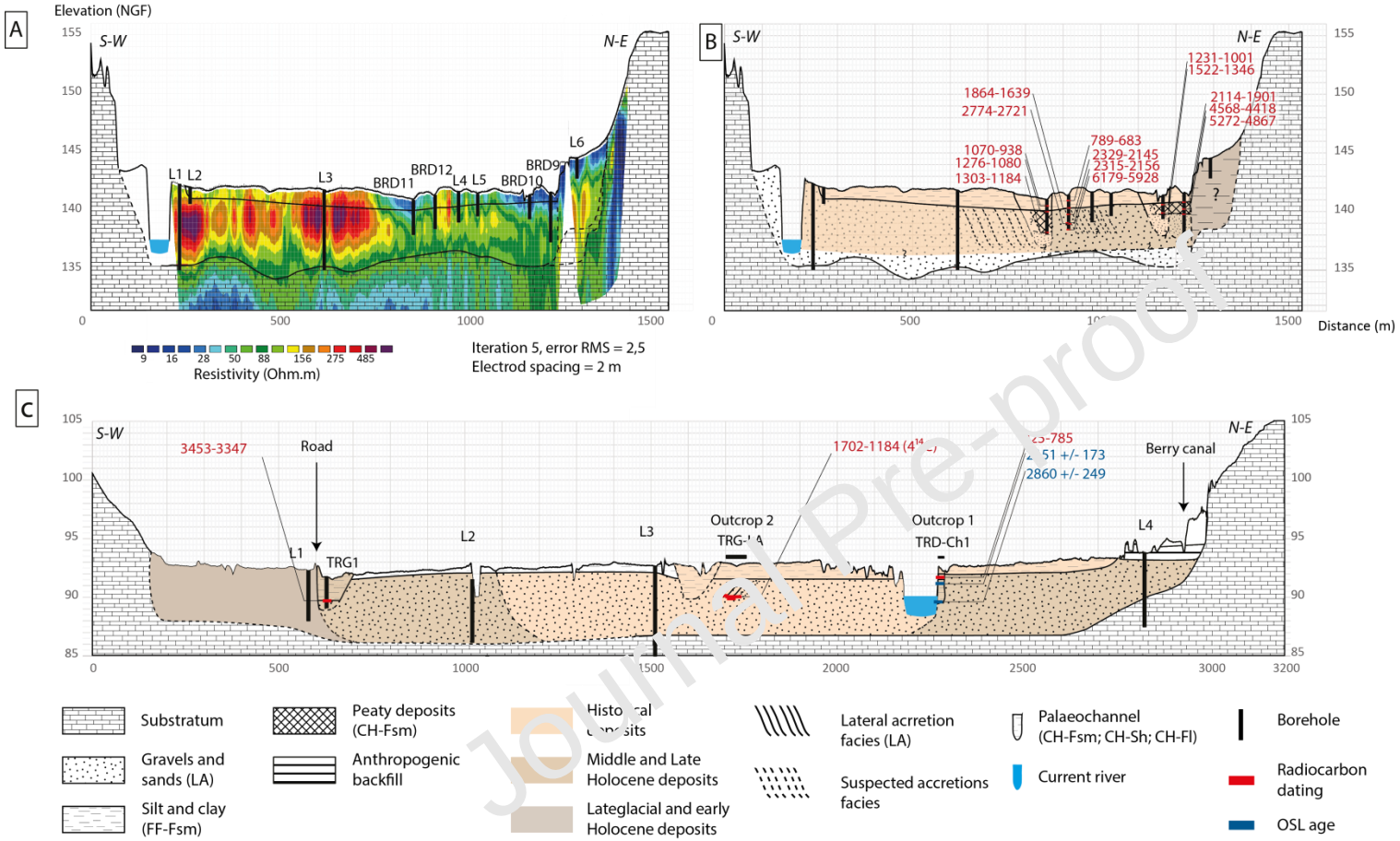

Fig. 4. Cross section of the valley. A. Geophysical survey and boreholes drilled in the Bigny floodplain. B Proposed sedimentary architecture of bedrock and alluvium at Bigny. C. Proposed sedimentary architecture of bedrock and alluvium at Thénioux. AMS-radiocarbon dates are presented as calibrated date 2 sigma (95.4%) cal. BP.

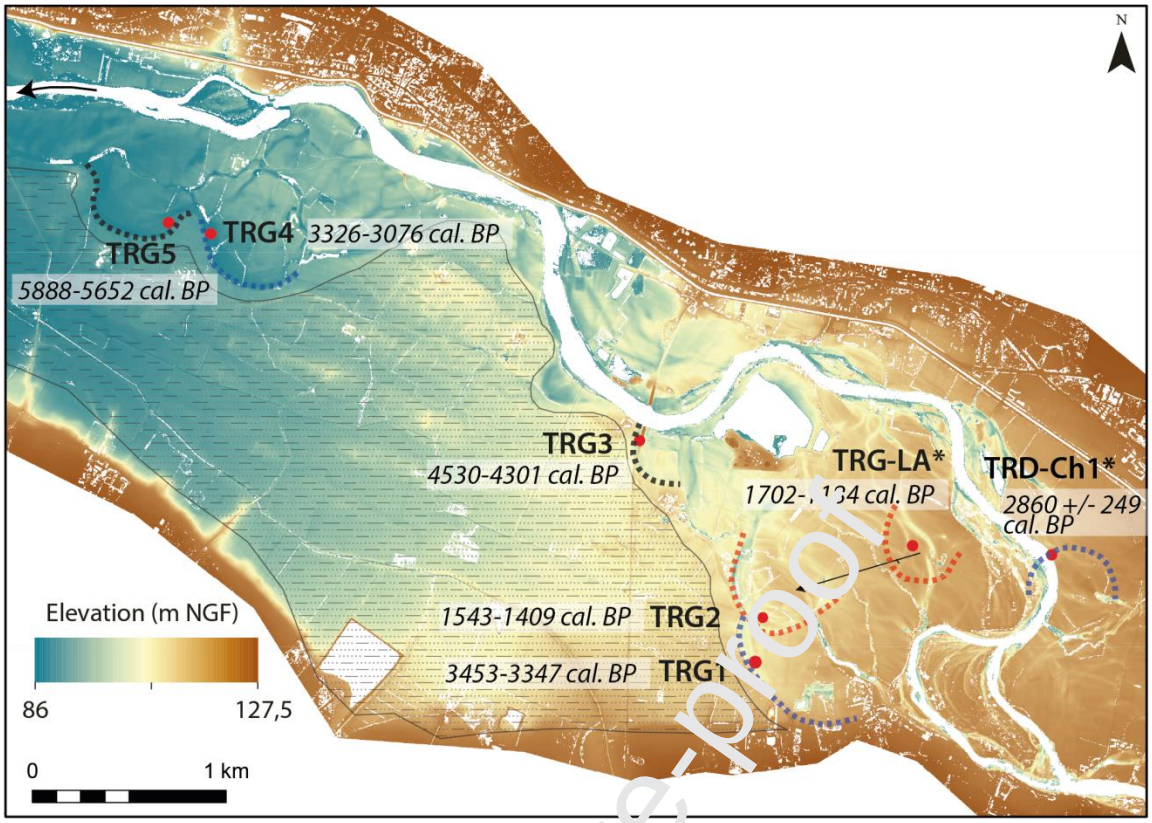

*Palaeomeanders identified at the base of outcrop surveys. Consequently, their paths are more uncertain compared to those identified through the LiDAR DEM.

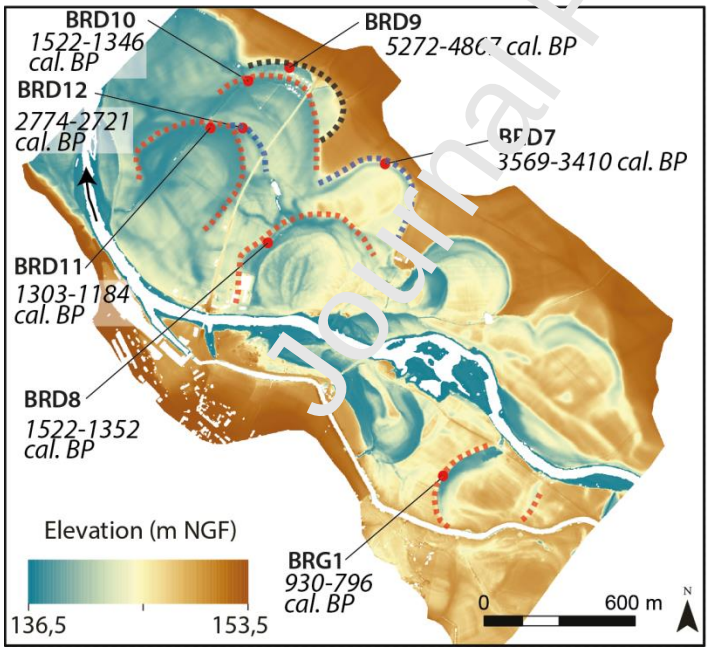

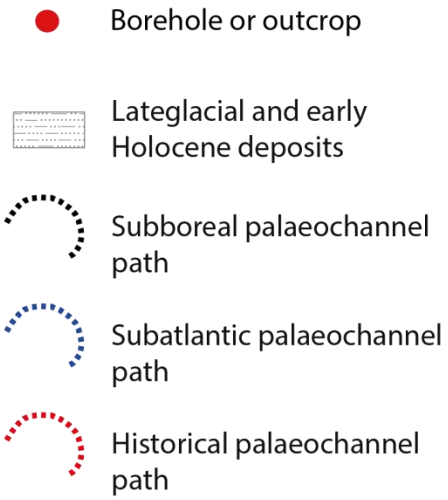

Fig. 5. Location and ages of palaeochannels. A. Thénioux reach; B. Bigny reach. AMS-radiocarbon dates are presented as calibrated date 2 sigma (95.4%) cal. BP.

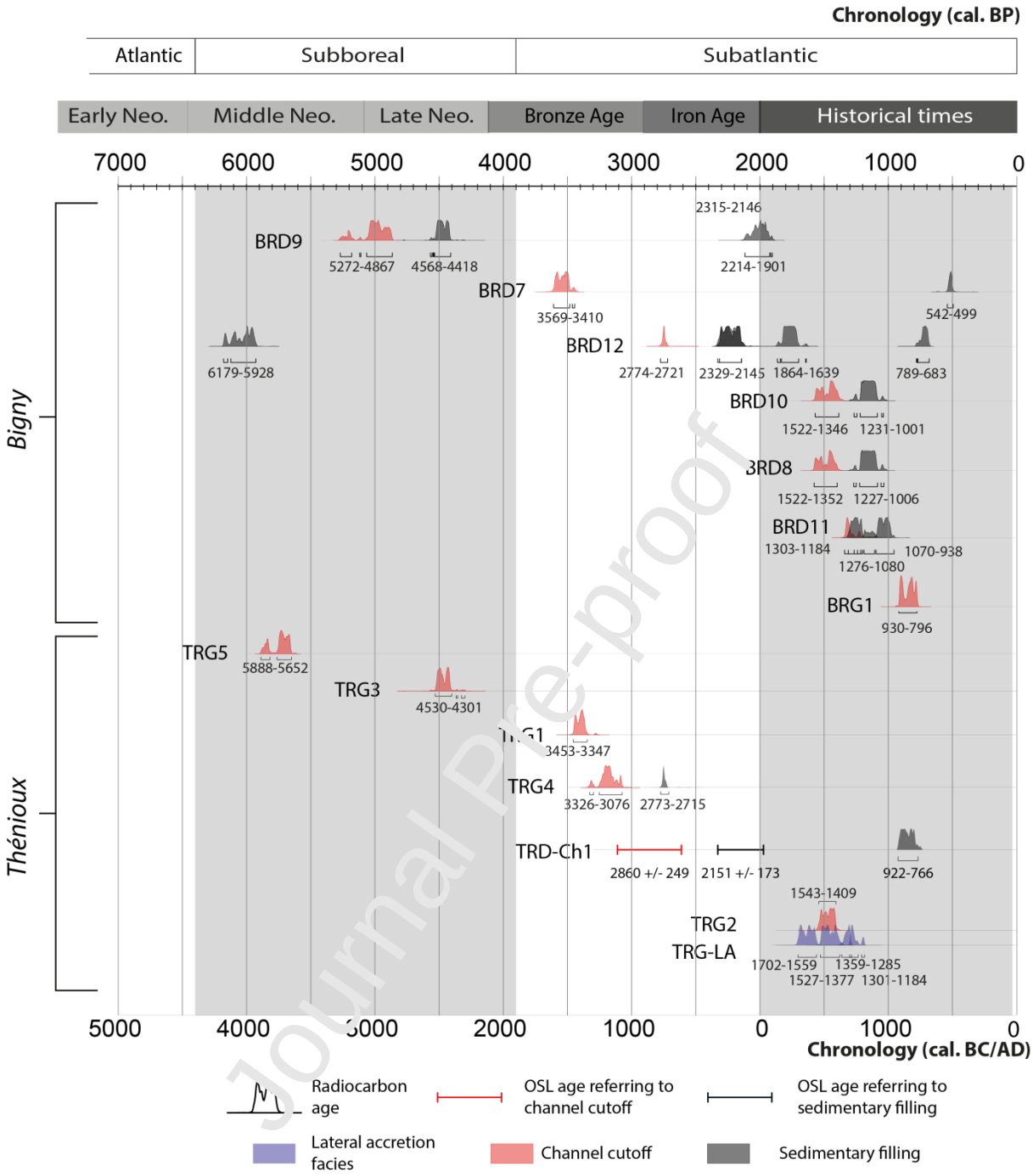

Fig. 6. Cutoff chronology. AMS-radiocarbon dates are presented as calibrated date 2 sigma (95.4 %) cal. BP. Chronozone: Visset et al. (2005). Archaeological chronology: Vannière and Martineau (2005).

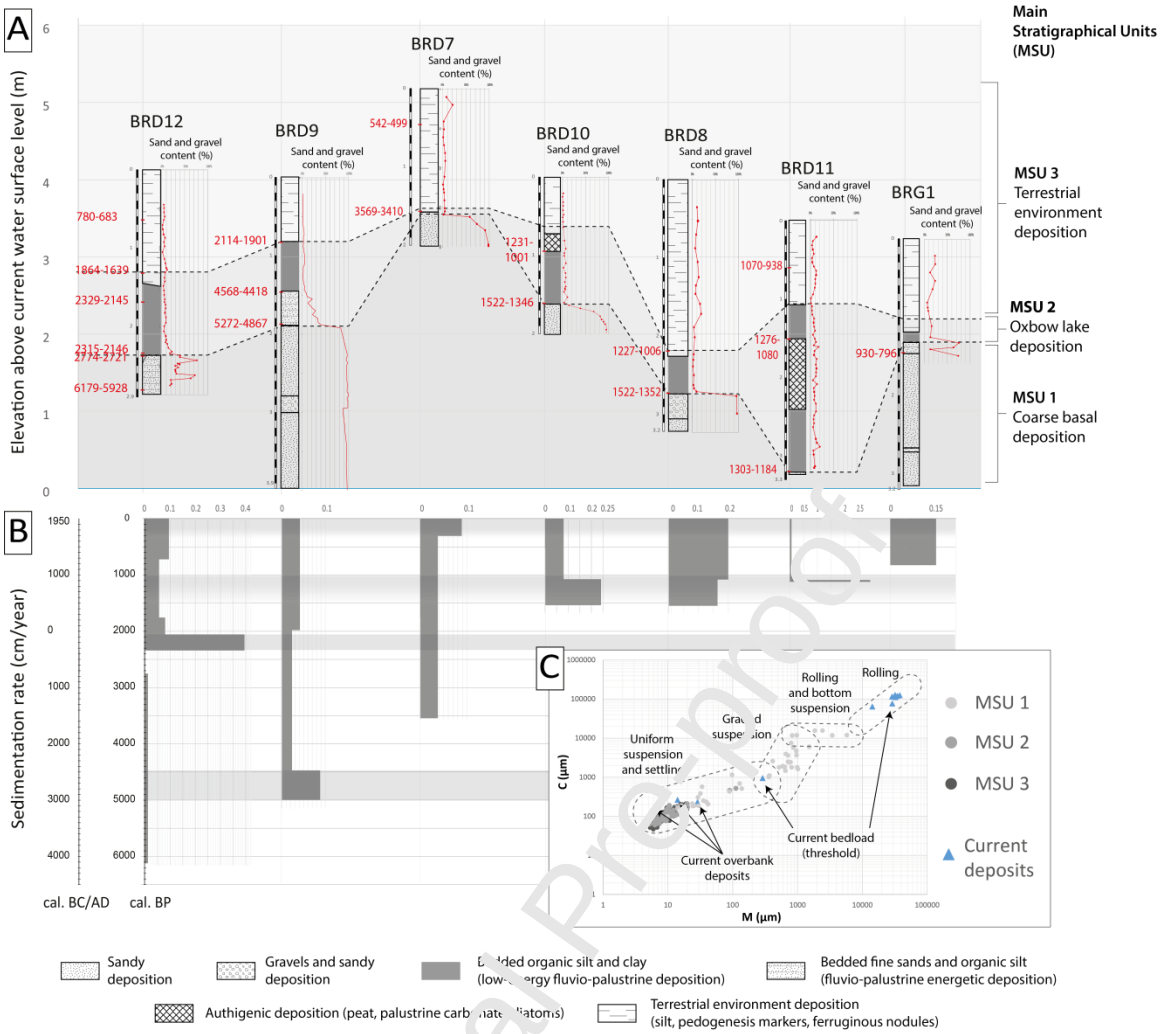

Fig. 7. Palaeochannel fill (Bigny). A. Palaeochannel fill and sand and gravel content. B. Sedimentation rates. C. CM diagram (adapted from Passega, 1957). AMS-radiocarbon dates are presented as calibrated date 2 sigma (95.4%) cal. BP.

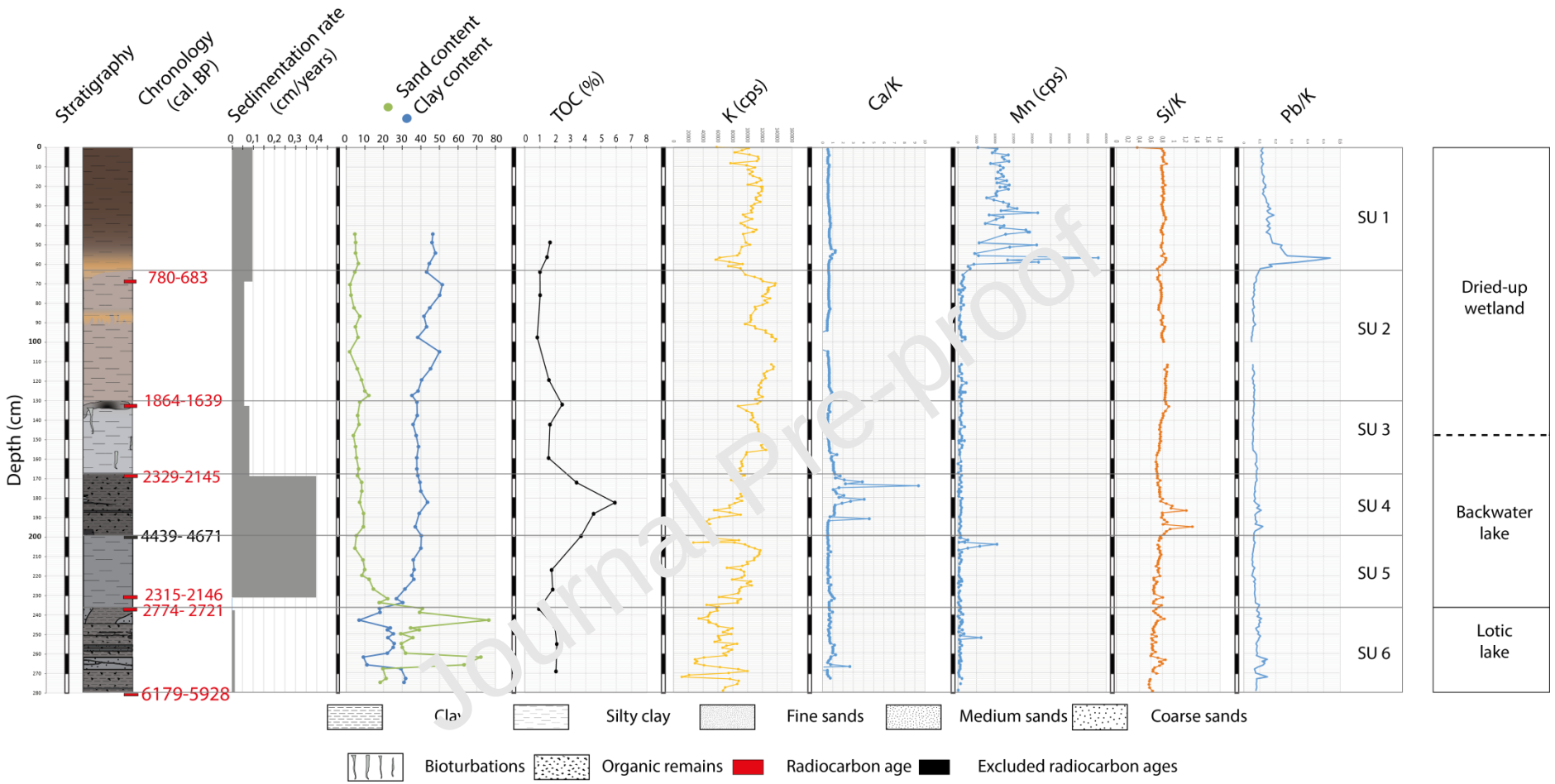

Fig. 8. Lithostratigraphic observations, grain size parameters and geochemical content

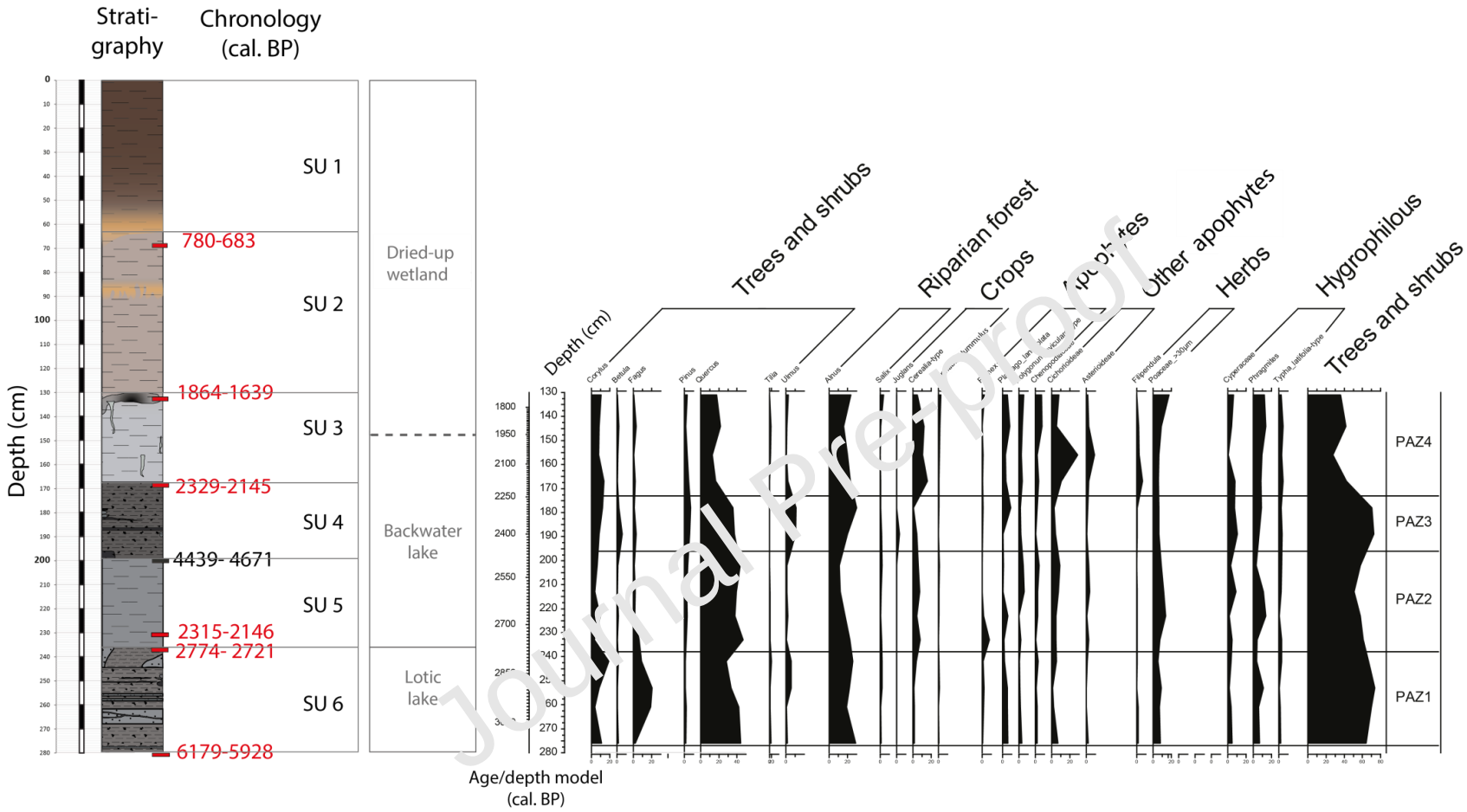

Fig. 9. Simplified pollen diagram of core BRD12. Pollen frequencies are expressed relative to the main pollen sum composed of trees and herbs; *Pinus*, helophytic and hydrophytic plants, *Pteridophyta* (monolete and trilete spores), and *Cyperaceae* were excluded from this main pollen sum. Riparian forest pollens, including *Alnus*, *Salix* and *Fraxinus* pollen grains were also excluded from the total pollen sum because they are usually over-represented in floodplain environments

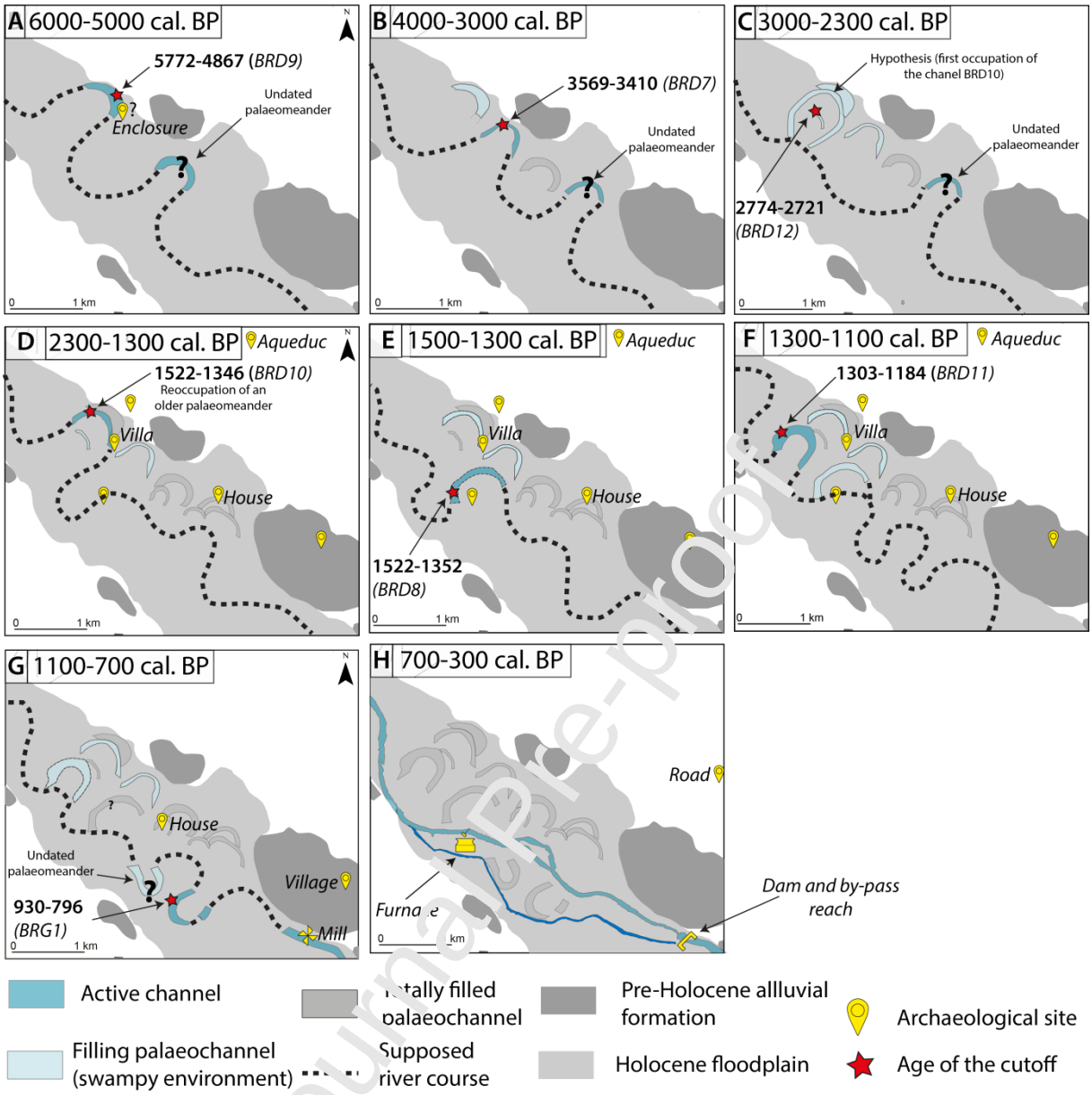

Fig. 10. Possible changes in lateral migration of the Cher River at Bigny (archaeological indications: Dumont et al., 2017; Gandini, 2006; Serna, 2013; Service Régional de l'Archéologie-Centre Val de Loire, 2017)

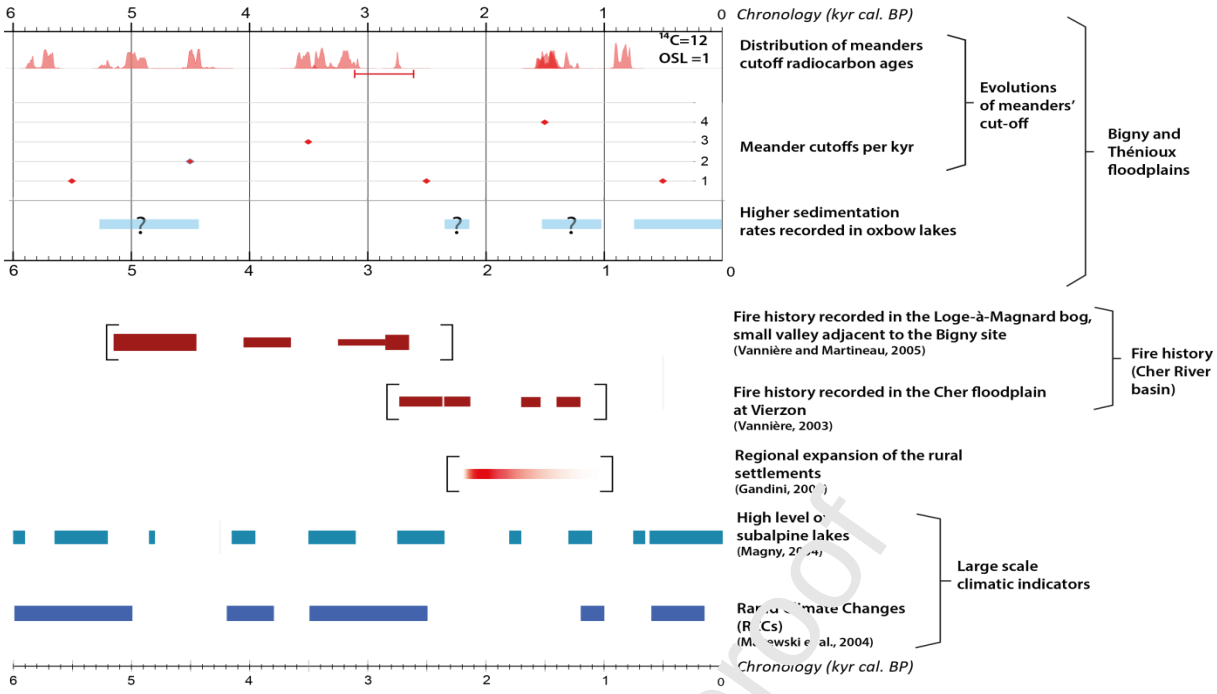

Fig. 11. Fluvial processes of the Cher River in the Bigny and Thénioux reaches compared with regional proxy (Gandini, 2006; Vannière, 2003; Vannière and Martineau, 2005) **and large-scale climate indicators** (Magny, 2004; Mayewski et al., 2004)**.**

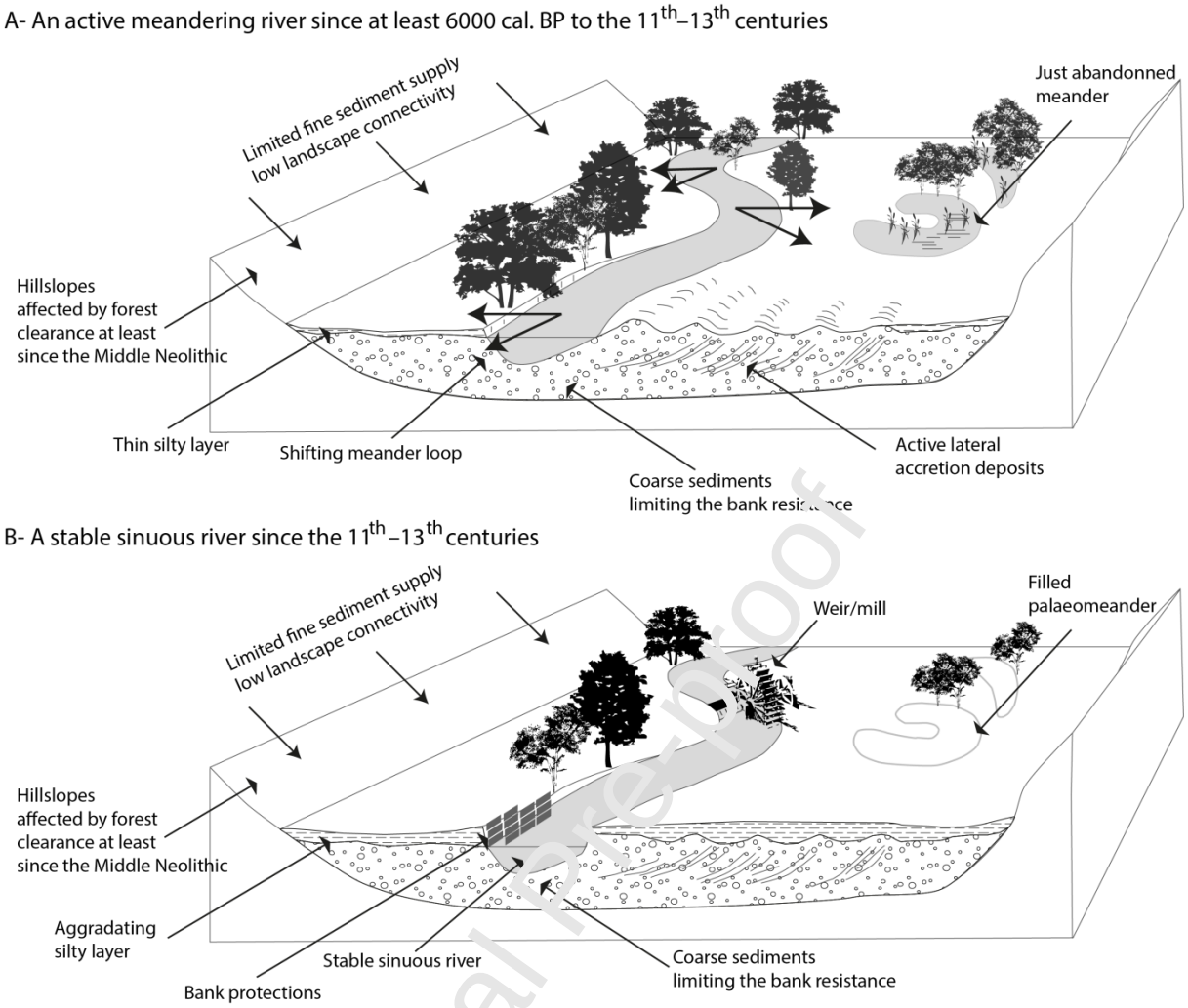

Fig. 12. Specific features associated with the two periods of meandering processes distinguished in the Cher River valley during the second half of the Holocene.

Table. 1. Main hydrological and morphological characteristics of the two study areas. The parameters marked with an asterisk are from Dépret (2014).

	Catchment area (km²)	Reach length studied (km)	Valley width (km)	Valley slope ($m.m^{-1}$)	Current mean annual discharge ($m^3.s^{-1}$)*	Current bankfull discharge ($m^3.s^{-1}$)*	Current bankfull width (m)*
Bigny	4100	4	1.2	0.00083	28.8	313	60
Thénioux	9070	8	1.7-2.8	0.0007	61.9	338	96

Table. 2. AMS-radiocarbon dates (calibration with OxCal v4.3.2 -Bronk Ramsey, 2009) according to the IntCal13 atmospheric curve (Reimer et al., 2013).

Sample code	Study area	Material	Core or outcrop	Location (Long; Lat)		Radiocarbon age (BP)	Calibrated date 2 sigma (95.4 %) (cal. BP)
Beta - 441215	Thénioux	Organic sediment	TRG5	1.8875142	47.2579941	5000 ± 30	5888-5652
DeA- 8877	Thénioux	Organic sediment	TRG3	1.92142	47.24887	3984 ± 34	4530-4301
Beta - 441216	Thénioux	Organic sediment	TRG1	1.92923	47.25897	3170 ± 30	3453-3347
Beta - 441214	Thénioux	Organic sediment	TRG4	1.8920015	47.2583162	3000 ± 30	3326-3076
DeA- 8886	Thénioux	Organic sediment	TRG2	1.9297	47.24104	1589 ± 29	1543-1409
DeA- 8895	Thénioux	Organic sediment	Outcrop 2	1.9407428	47.2441861	1330 ± 29	1301-1184
Beta - 440280	Thénioux	Organic sediment	Outcrop 2	1.9405732	47.2440675	1550 ± 30	1527-1377
Beta - 440282	Thénioux	Organic sediment	Outcrop 2	1.940665	47.2441044	1410 ± 30	1359-1285
Beta - 440281	Thénioux	Organic sediment	Outcrop 2	1.9408348	47.244214	1720 ± 30	1702-1559
Beta-448858	Thénioux	Trunk	Outcrop 1	1.9500216	47.2436313	4960 ± 30	5742-5608
Beta - 459240	Thénioux	Trunk	Outcrop 1	1.949955	47.2436577	7390 ± 30	8324-8165
Beta - 459239	Thénioux	Trunk	Outcrop 1	1.94844	47.2445999	3300 ± 30	3592-3453
Beta - 459241	Thénioux	Trunk	Outcrop 1	1.9486155	47.2445459	3110 ± 30	3386-3237
Beta - 459238	Thénioux	Charcoal	Outcrop 1	1.94995	47.24364	920 ± 30	922-766
Poz-72120	Bigny	Wood remains	BRD10	2.37361	46.81345	1525 ± 35	1522-1346
Poz-74381	Bigny	Wood remains	BRD10	2.37361	46.81345	1195 ± 30	1231-1001
Poz-72072	Bigny	Organic sediment	BRD9	2.37584	46.81389	4415 ± 35	5272-4867
Poz-77554	Bigny	Organic sediment	BRD9	2.37584	46.81389	4000 ± 35	4568-4418

Poz-77937	Bigny	Organic sediment	BRD9	2.37584	46.81389	2040 ± 35	2114-1901
Poz-72130	Bigny	Wood remains	BRD12	2.37332	46.81177	5255 ± 35	6179-5928
Poz-77553	Bigny	Organic sediment	BRD12	2.37332	46.81177	2610 ± 30	2774-2721
DeA- 8887	Bigny	Organic sediment	BRD12	2.37332	46.81177	2202 ± 28	2315-2146
Poz-77567	Bigny	Organic sediment	BRD12	2.37332	46.81177	3910 ± 35	4439- 4671
Poz-77566	Bigny	Organic sediment	BRD12	2.37332	46.81177	2210 ± 35	2329-2145
Poz-75193	Bigny	Organic sediment	BRD12	2.37332	46.81177	1830 ± 30	1864-1639
DeA- 8881	Bigny	Organic sediment	BRD12	2.37332	46.81177	812 ± 26	780-683
Poz-77941	Bigny	Organic sediment	BRD11	2.37111	46.81172	1335 ± 30	1303-1184
DeA- 8893	Bigny	Organic sediment	BRD11	2.37111	46.81172	2564 ± 30	2755-2596
DeA- 8891	Bigny	Organic sediment	BRD11	2.37111	46.81172	1252 ± 32	1276-1080
Poz-77938	Bigny	Organic sediment	BRD11	2.37111	46.81172	5810 ± 50	6734-6494
DeA- 8890	Bigny	Organic sediment	BRD11	2.37111	46.81172	1110 ± 29	1070-938
Beta - 440279	Bigny	Organic sediment	BRD8	2.37469	46.80763	1190 ± 30	1227-1006
Poz-75195	Bigny	Organic sediment	BRD8	2.37469	46.80763	1530 ± 30	1522-1352
DeA- 8874	Bigny	Organic sediment	BRG1	2.38401	46.79926	962 ± 28	930-796
Beta - 440278	Bigny	Organic sediment	BRD7	2.3808	46.8105	480 ± 30	542-499
DeA- 8872	Bigny	Organic sediment	BRD7	2.3808	46.8105	3267 ± 29	3569-3410

Table 3. Optically stimulated luminescence (OSL) measurements made in Thénioux.

Sample code	Depth below the current surface (m)	Location (Long; Lat)		Palaeo-dose(Gy)	Dose rate (Gy/ka)	Optical Age (yr)
LS1771	1.85	1.94863	47.24456	6.7 ± 0.30	3.694±0.221	1814 ± 145
LS1772	2	1.94941	47.24428	5.9 ± 0.26	2.719±0.188	2170 ± 189
LS1773	1.5	1.94973	47.24393	6.93 ± 0.24	3.010±0.179	2303 ± 172
LS1774	2.6	1.94993	47.2437	8.2 ± 0.26	2.867±0.217	2860 ± 249
LS1775	3	1.94992	47.24373	14.6 ± 0.38	2.70±0.209	5407 ± 469
LS1776	1.5	1.94992	47.24373	19.3 ± 0.51	3.969±0.232	4862 ± 342
LS1777	1.1	1.94993	47.2437	7.2 ± 0.32	3.347±0.203	2151 ± 173

Table. 4. Lithofacies of the stratigraphic units

SU	*Lithofacies (Miall, 1996)*	*Description*	*D50 (µm)*	*D99 (µm)*	*TOC (%)*	*Depositional environment*	*Transport processes*
1	**CH-Fsm/P**	Brown silty clay	7.6 >M> 8.4	89.6 >C> 128.2	1 >TOC> 1.65	Dried-up wetland	Uniform suspension
2	**CH-Fsm/P**	Brown silty clay, pedogenesis markers	6.8 >M> 12	69.4 >C> 139.15	0.8 >TOC> 1.6	Dried-up wetland	Uniform suspension
3	**CH-Fsm/P**	Brown silty clay, pedogenesis markers	10.2 >M> 11.5	77.8 >C> 120.4	1.55 >TOC> 2.1	Dried-up wetland	Uniform suspension
4	**CH-Fl/C**	Bedded grey silty clay, slightly sandy, organic remains, palustrine carbonates	8.8 >M> 10.5	97.4 >C> 128.7	3.4 >TOC> 5.9	Wetland filled by overbank deposit, organic matter and palustrine carbonates	Uniform suspension
5	**CH-Fsm**	Bedded grey silty clay, slightly sandy	9.7 >M> 20	99.8 >C> 171.9	1.75 >TOC> 3.7	Wetland filled by overbank deposit and organic matter	Uniform suspension
6-1	**CH – Fsm**	Grey clay and bedded fine sands	41 >M> 138	204 >C> 513	~1%	Chute channel connected during low-magnitude flood	Graded suspension
6-2	**CH-Sh/Fl**	Bedded clay, fine sands and organic remains	23.9>M> 35.2	182,6 >C> 383	~2%	"	Uniform suspension/graded suspension
6-3	**CH- Sm**	Fine and medium sands	89 >M>127.8	433.8 >C> 690.2	~2%	"	Graded suspension
6-4	**CH- Sh**	Bedded clay, fine sands and organic remains	9.8 >M> 17.4	99.8 >C> 189.7	~2%	"	Uniform suspension/graded suspension

Table. 5. Durations of floodplain turnover and speed of recycling based on the palaeomeanders of Bigny

	Distance from the existing river inherited of the 11th-13th centuries (m)	Age of the cutoff according to the confidence interval (yr cal. BP)		Length of time between the cutoff and the stabilization of the existing river (yr)		Speed of reworking extend ($m.yr^{-1}$)		Theoretical duration of the floodplain turnover (yr)		Measured duration of the floodplain turnover (yr)	
		Maximum	Minimum	Maximum	Minimum	Minimum	Maximum	Minimum	Maximum	Minimum	Maximum
BRD11	715.721	1303	1184	553	234	1.29	3.06	357.52	844.92	_	_
BRD9	1093.534	5272	4867	4522	3917	0.22	0.28	_	_	3917	4522
BRD8	562.543	1522	1352	772	402	0.42	1.40	615.43	1181.87	_	_
BRD7	861.21	3569	3410	2819	2460	0.25	0.35	_	_	2460	2819

Declaration of competing interests

☐ The authors declare that they have no known competing financial interests or personal relationships that could have appeared to influence the work reported in this paper.

☐The authors declare the following financial interests/personal relationships which may be considered as potential competing interests: